FINAL PROJECT REPORT #00050028

GRANT: DTRT13-G-UTC45
Project Period: 1/1/2015 – 5/15/17

Influence of Casting Conditions on Durability and Structural Performance of HPC-AR: Optimization of Self-Consolidating Concrete to Guarantee Homogeneity during Casting of Long Structural Elements

Participating Consortium Member:
Missouri University of Science and Technology

Authors:

Dimitri Feys, Ph.D.
Assistant Professor
Dept. of Civil, Arch. & Environ. Engineering
Missouri S&T

Aida Margarita Ley Hernandez
M.S. Student
Dept. of Civil, Arch. & Environ. Engineering
Missouri S&T

RE-CAST:
REsearch on Concrete Applications for Sustainable Transportation
Tier 1 University Transportation Center

DISCLAIMER

The contents of this report reflect the views of the authors, who are responsible for the facts and the accuracy of the information presented herein. This document is disseminated under the sponsorship of the U.S. Department of Transportation's University Transportation Centers Program, in the interest of information exchange. The U.S. Government assumes no liability for the contents or use thereof.

TECHNICAL REPORT DOCUMENTATION PAGE

1. Report No. RECAST UTC #00050028	**2. Government Accession No.**	**3. Recipient's Catalog No.**
4. Title and Subtitle Influence of Casting Conditions on Durability and Structural Performance of HPC-AR: Optimization of Self-Consolidating Concrete to Guarantee Homogeneity during Casting of Long Structural Elements		**5. Report Date** May 2017 **6. Performing Organization Code:**
7. Author(s) D. Feys and A.M. Ley Hernandez		**8. Performing Organization Report No.** Project #00050028
9. Performing Organization Name and Address RE-CAST – Missouri S&T 500 W. 16th St., 223 Engineering Research Lab Rolla, MO 65401		**10. Work Unit No.** **11. Contract or Grant No.** USDOT: DTRT13-G-UTC45
12. Sponsoring Agency Name and Address Office of the Assistant Secretary for Research and Technology U.S. Department of Transportation 1200 New Jersey Avenue, SE Washington, DC 20590		**13. Type of Report and Period Covered:** Final Report Period: 1/1/2015 – 5/17/17 **14. Sponsoring Agency Code:**
15. Supplementary Notes The investigation was conducted in cooperation with the U. S. Department of Transportation.		
16. Abstract This report is a summary of the research done on dynamic segregation of self-consolidating concrete (SCC) including the casting of pre-stressed beams at Coreslab Structures. SCC is a highly flowable concrete that spreads into place with little to no mechanical vibration [1]. The high fluidity of the concrete is achieved by the addition of special construction chemicals, called superplasticizers. One of the main challenges for SCC is to combine the high flowability and passing ability with stability: the concrete must remain homogeneous during production, transport and placement. Settling of the aggregates or rising of cement paste or bleeding water could lead to inferior properties in parts of the structure [2]. Segregation can be static when the mixture separates at rest, or dynamic, when the aggregates sink during flow.		
17. Key Words Dynamic segregation, self-consolidating concrete, adapted rheology	**18. Distribution Statement** No restrictions. This document is available to the public.	
19. Security Classification (of this report) Unclassified	**20. Security Classification (of this page)** Unclassified	**21. No of Pages** 75

Form DOT F 1700.7 (8-72) Reproduction of form and completed page is authorized.

Table of Contents

1 Introduction

This report is a summary of the research done on dynamic segregation of self-consolidating concrete (SCC) including the casting of pre-stressed beams at Coreslab Structures. SCC is a highly flowable concrete that spreads into place with little to no mechanical vibration [1]. The high fluidity of the concrete is achieved by the addition of special construction chemicals, called superplasticizers. One of the main challenges for SCC is to combine the high flowability and passing ability with stability: the concrete must remain homogeneous during production, transport and placement. Settling of the aggregates or rising of cement paste or bleeding water could lead to inferior properties in parts of the structure [2]. Segregation can be static when the mixture separates at rest, or dynamic, when the aggregates sink during flow.

The goal of this research is to better understand the mechanisms that influence dynamic segregation in SCC. In this way, practical guidelines are developed to avoid the negative consequences of dynamic segregation on the performance of prestressed beams, in terms of mechanical properties, durability and bond strength with pre-stress strands. This report focuses on the influence on dynamic segregation of the different mix design factors which can be varied based on the materials available at Coreslab Structures and the influence of dynamic segregation on the compressive strength of cores and the bond strength of prestress strands. Seen the high number of cores sampled, the sorptivity tests and hardened air void analyses are still ongoing and will be provided as an addendum to this report, once finished.

In this report, a summary of the available literature on dynamic segregation is given, focusing on several testing apparatuses and on mix design parameters influencing dynamic segregation. In the following section, the influence of concrete mix design on dynamic segregation is discussed, based on three series of SCC mixtures produced in the lab. Section 4 discusses the full-scale casting tests at Coreslab Structures focusing on the consequences of dynamic segregation on compressive strength of cores and bond strength of prestress strands. Finally, the results are summarized and practical recommendations are given.

1.1 Self-Consolidating Concrete

Self-Consolidating Concrete (SCC) has been developed in the 1980s in Japan to counteract the lack of skilled workers to perform the consolidation [3]. The philosophy was to produce concrete which could self-consolidate by gravity alone, eliminating the need for vibration and all problems associated with inadequate consolidation. Furthermore, SCC needs to possess three basic properties [1] [4] [5]:

- Filling ability, requiring SCC to fill the formwork entirely without the need of external forces.
- Passing ability, which imposes that SCC must be able to flow through narrow gaps, created by the formwork, or by the reinforcement.
- Stability, which means that the SCC must remain homogeneous during production, transport and placement.

Achieving these three basic properties at the same time is the challenge in producing SCC, as the filling and passing ability require a very fluid, water-like material, while the material cannot be too fluid to assure sufficient stability.

Typically, the high fluidity of SCC is obtained by incorporating superplasticizers (SP), eliminating the need to increase the amount of water, which would reduce the quality of the concrete. The passing ability is usually achieved by reducing the maximum aggregate size and by reducing the amount of coarse aggregates, compared to conventional vibrated concrete. In this way, the chance to form granular arches in narrow channels, and thus blocking, is reduced. Providing sufficient stability can be achieved in several ways, but the main strategy is to increase the stickiness of the concrete. This can be achieved by lowering the amount of water, relative to the amount of fines: typically, the amount of fines, by incorporating more SCMs or

mineral fillers, is increased. A second strategy is to increase the stickiness of the concrete by using viscosity-modifying agents (VMA), which immobilize a part of the water or a part of the cement particles. Optimizing the aggregate gradation, to enhance the particle lattice effect, has also proven to be a valuable strategy in enhancing stability without compromising the filling and passing ability [6].

1.2 Rheology

Rheology is per definition the science of deformation of matter [7]. For fresh concrete, which is considered as a liquid material, the material can be characterized by finding the relationship between the shear stress (τ), typically expressed in Pa, and the shear rate ($\dot{\gamma}$), expressed in s^{-1} [8]. The shear stress is well related to a force, torque or pressure applied, potentially just by gravity, to move the material. The shear rate, which is a velocity gradient, is well related to the flow velocity and the width of the channel where the material flows through. Fresh concrete is generally found to be a Bingham material, having a yield stress (τ_0, in Pa) and a plastic viscosity (μ_p, in Pa s) (eq. 1, Figure 1) [8]. The yield stress is the stress which needs to be exceeded to start flow, while the plastic viscosity is the resistance to an increase in velocity or flow rate. In simple terms, the yield stress is very well correlated to the slump or slump flow of concrete, while the viscosity is mostly expressed as the stickiness.

$$\tau = \tau_0 + \mu_p \dot{\gamma} \qquad \textit{(eq.1)}$$

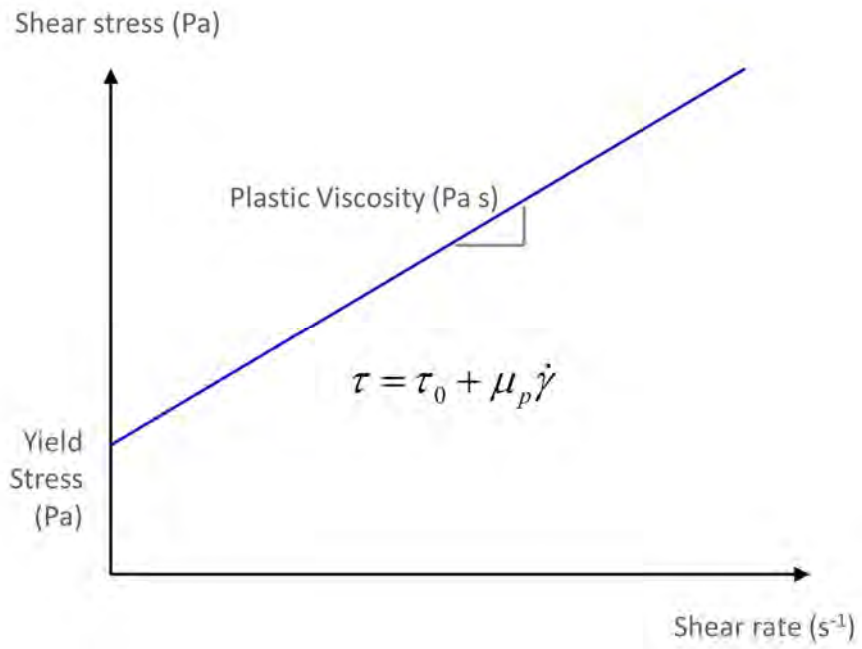

Figure 1. Representation of the Bingham model, defining yield stress and plastic viscosity.

However, the behavior of fresh concrete is more complex and depends on elapsed time and on previously applied flow conditions. Thixotropy, which is the stiffening of concrete at rest without setting, and workability loss, which is the consequence of hydration reactions in the dormant period, cause the yield stress and plastic viscosity of concrete to change with time [9] [10]. To minimize the impact of these variations within the testing time, the research team has selected a SP with long workability retention for the first part of the research work, which is less typical for the pre-cast industry. In the second part, and for the work conducted at Coreslab Structures, an efficient SP was used, but the admixture had short workability retention.

2 Summary of Literature on Dynamic Segregation

In this section of the report, a brief overview of the different test methods which have been developed to evaluate dynamic segregation is given. Based on the results of two studies [11] [12], the influence of different mix design parameters is discussed. Most other studies performed on dynamic segregation indicate similar trends.

2.1 Definition

"Stability is the capacity of concrete to remain homogeneous during mixing, transportation and placement. [1]*"* Segregation is, logically, the opposite and will lead to an inhomogeneous distribution of constituent elements over the height, and potentially the length and width, of the cast specimen. Usually, segregation causes the coarse aggregates to sink and/or the cement paste (or water) to float on top of the surface.

Static segregation occurs when concrete is at rest. It is usually determined by means of the column segregation test [13] (North-America) or the sieve stability test [5] (Europe). Dynamic segregation occurs during flow, whether the flow is horizontal or vertical, the latter referring to the influence of dropping the concrete. No standardized test methods for dynamic segregation are available. The following section reviews different methods to assess dynamic segregation, discussed in the literature.

2.2 Test Methods

In this section, a brief overview is given of different test methods to assess dynamic segregation, their modus operandi and the criterion to distinguish between stable and segregated concrete, if applicable.

2.2.1 Visual Stability Index

The visual stability index (VSI) [14] is determined in parallel with the slump flow and T_{50} of SCC. Evaluating the concrete spread will lead to a value between 0 and 3, based on a predefined table with pictures and descriptions. A VSI of zero indicates stable SCC, while three means severe segregation. The VSI can be interpreted as a simple dynamic segregation test, as the concrete effectively flows, but the flow distance and velocity are restricted. Furthermore, no actual measurement is taken, making the VSI a subjective assessment technique.

2.2.2 Flow trough

The flow trough is a rectangular channel: 150 x 150 x 1800 mm (6 x 6 x 31.5 in.) inclined to assure a height difference of 230 mm (9 in.) (Figure 2) [15]. The content of one 150 x 300 mm (6 x 12 in.) cylinder is poured in the trough to precondition the flow plane. As the trough is held vertically for 30 s, a layer of cement paste or mortar is left on the trough surfaces. After the trough is placed back in its initial, inclined position, the contents of a second 150 x 300 mm (6 x 12 in.) cylinder is poured. The leading portion of the concrete is captured at the end of the trough in a 100 x 200 mm (4 x 8 in.) cylinder. The coarse aggregate content retained on a #4 sieve of this latter cylinder is compared to the coarse aggregate content in a 100 x 200 mm (4 x 8 in.) cylinder taken directly from the concrete batch (reference cylinder). Dynamic segregation is calculated as the difference between the coarse aggregate contents in both cylinders, divided by the coarse aggregate content in the reference cylinder. According to the authors, the stability criterion depends on several mix design factors: no unique value is identified [15].

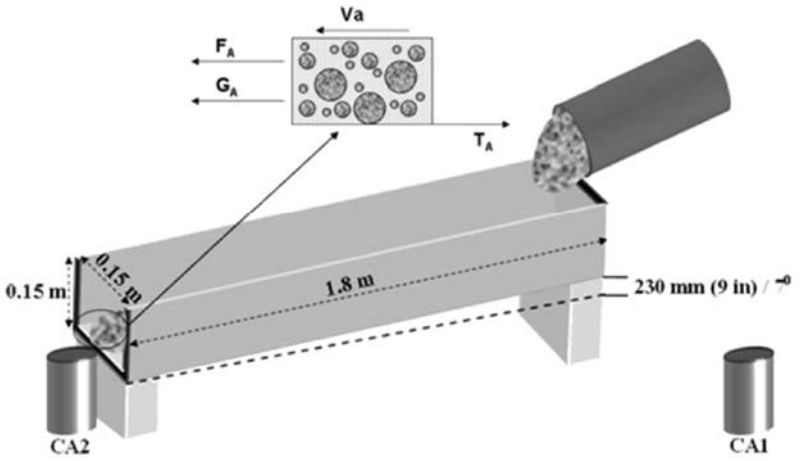

Figure 2. Flow trough for dynamic segregation [15].

2.2.3 Penetration test used with L-box

Segregation can be assessed by performing the L-box test [5]. After filling the vertical leg of the L-box, a penetration apparatus, with a mass of 54 g (0.12 lbs) is placed on the concrete surface and allowed to penetrate the concrete during 45 s (Figure 3) [16]. The L-box test is then performed to determine the filling and passing ability of the concrete and a sample of concrete is taken at both ends of the L-box. The samples fill an 80 x 70 mm (3.15 x 2.75 in.) cylinder each and are washed on a 3/8 in. sieve. If the penetration is larger than 9 mm (0.35 in.) or the difference in aggregate content in both cylinders is larger than 10%, dynamic segregation has occurred.

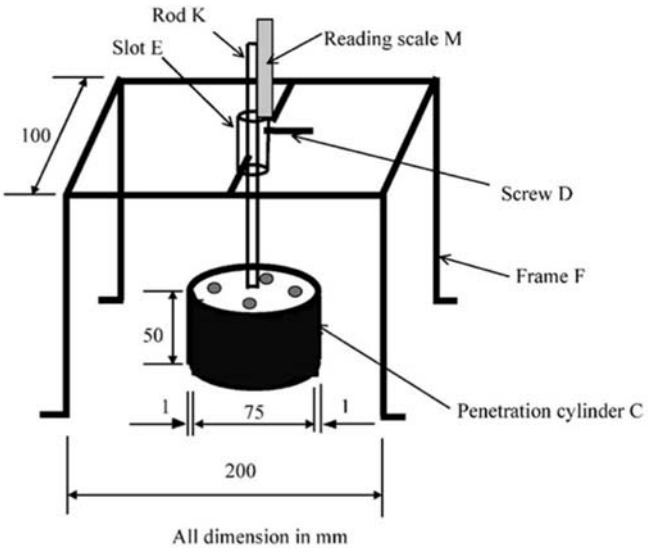

Figure 3. Penetration apparatus used in combination with L-box [16].

2.2.4 Modified penetration depth apparatus

A modified version of the penetration apparatus described above was developed by El-Chabib and Nehdi [12]. The penetration apparatus itself consists of four penetration heads with a semi-spherical end, each approximately 25 g (0.055 lbs) in mass and 20 mm (0.8 in.) in diameter, mounted on a rigid frame (Figure 4 right). Concrete is placed in a modified 150 x 300 mm (6 x 12 in.) cylinder and the penetration apparatus is

placed on top of the concrete. The cylinder itself consists of three sections, each 150 x 100 mm (6 x 4 in.) (Figure 4 left). After letting the concrete rest for 30 min, the coarse aggregate content, retained on a 9.5 mm sieve (3/8 in.), is determined for each section. Segregation occurs if the coefficient of variation of the coarse aggregate content is larger than 10%. In order to evaluate dynamic segregation, the concrete sample in the 150 x 300 mm (6 x 12 in.) cylinder is taken flowing out of the V-Funnel test. In this case, a flow and a drop height additionally influence segregation resistance.

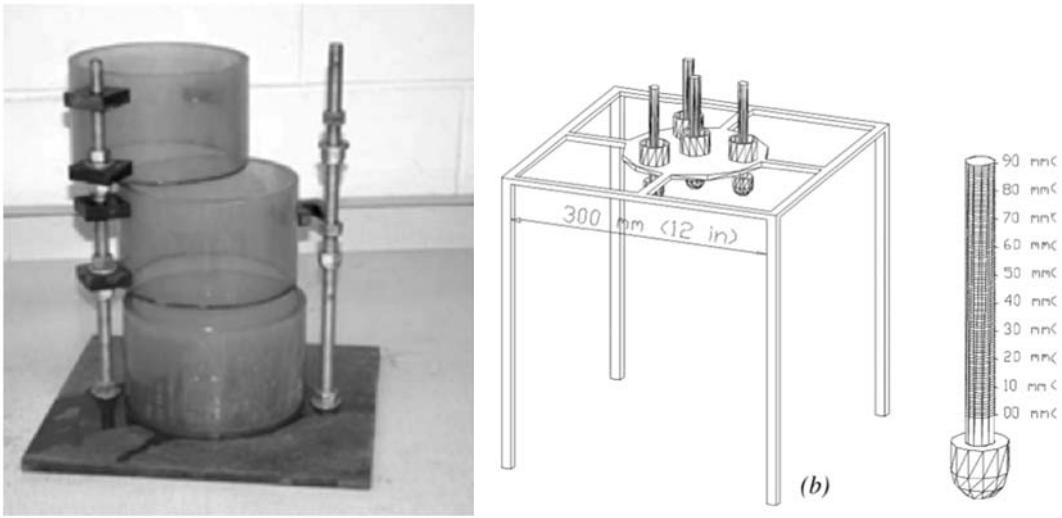

Figure 4. Modified cylinder (left) and modified penetration device (right) developed by El-Chabib and Nehdi [12].

2.2.5 Modified L-box apparatus

In order to evaluate dynamic segregation, Turgut et al. [17] modified the L-box test by inserting three partitions. After performing the L-box test, the partitions are inserted to isolate three different sections in the L-box (Figure 5). The volume of coarse aggregates is determined in each section and compared to the volume of concrete in the respective section. Statistical analysis, for which more details can be found in [17], determines the segregation coefficient.

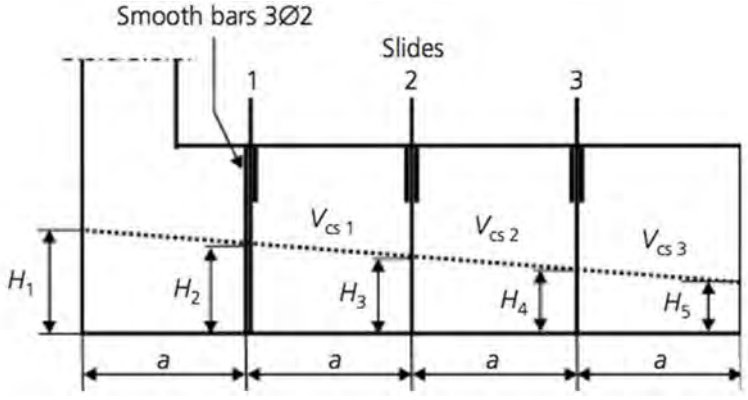

Figure 5. Modified L-box with partitions developed by Turgut et al. [17].

2.2.6 Tilting box (T-box)

The tilting box is used to evaluate dynamic segregation of SCC [11] [18]. It consists of a rectangular channel of 1 m (3.3 ft) long which can tilt from a horizontal to an inclined position (Figure 6 and Figure 7). The tilting

height of the box is 140 mm (5.5 in.). The box at Missouri S&T has a width of 400 mm (15.75 in.), which can be divided into two sections: one with a width of 100 mm (4 in.), and one with 200 mm (8 in.) width [19]. Before testing, fresh concrete is placed reaching a height of 80 mm (3.15 in.) in both sections, while the box was maintained in horizontal position. The box is then tilted during 1 second, and brought back to horizontal during another second. Cycle time can be varied during the test, but in this testing program, the cycle time is kept constant at 2s.

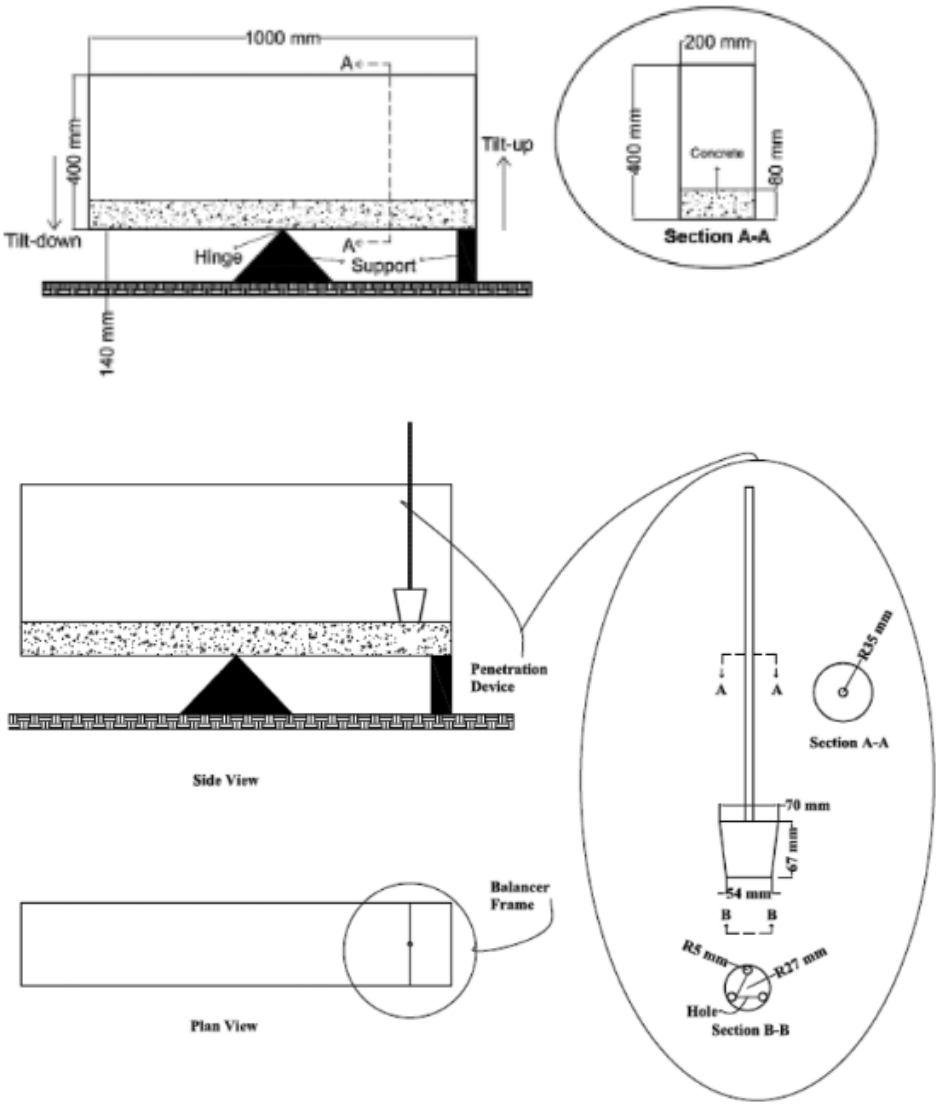

Figure 6. Schematic representation of tilting box (without subdivision channels) and penetration device [18].

Before the test, and after 30, 60, 90 and 120 cycles, segregation was assessed with the penetration device, measuring how deep the tool sinks in the concrete which is in the “tilt-up” section (Figure 6). When tilting down, the aggregates are expected to follow the mortar during flow, as gravity pulls them towards the down section. When tilting back to the horizontal position, the mortar has to drag the aggregates back into the original position, which is more difficult. If insufficient drag is executed on the aggregates, more aggregates

will assemble in the tilt-down section. As more mortar or paste is in the tilt-up section, a larger penetration is expected with an increased number of cycles.

After completing 120 cycles, which corresponds theoretically to a flow distance of 9 m (30 ft), samples are taken from the tilt-up and tilt-down sections, from both the 100 (4 in.) and 200 mm (8 in.) width channels. Standard 100 x 200 mm (4 x 8 in.) cylinders were filled with concrete, washed over a No. 4 sieve, and dried to measure the amount of coarse aggregates in each of the sample sections. The amount of aggregate in each section directly corresponds to dynamic segregation. This measurement is expressed as the Volumetric Index (VI) (eq. 2), where V_{td} is the relative coarse aggregate volume in the tilt-down section and V_{tu} is the relative coarse aggregate volume in the tilt-up section.

$$VI(\%) = 100\frac{V_{td} - V_{tu}}{average(V_{td}, V_{tu})} \qquad \textit{(eq.2)}$$

Figure 7. Tilting box [19].

Dynamic segregation occurs, according to [18], when the volumetric index is larger than 25%. This value is confirmed based on the results in this report.

2.2.7 Dynamic sieve stability test

A modification of the tilting box test is the dynamic sieve stability test [20]. It consist of a box, similar to the tilting box, but the bottom of the box is a mesh with 6 mm (0.24 in.) opening (Figure 8). A total of 18 kg (40 lbs) is poured in the box, and the box is cycled 4 times, taking 15 s per cycle. Dynamic segregation is

measured as the mass of concrete fallen through the mesh, relative to the initial mass of concrete. A maximum segregation index of 30% is recommended.

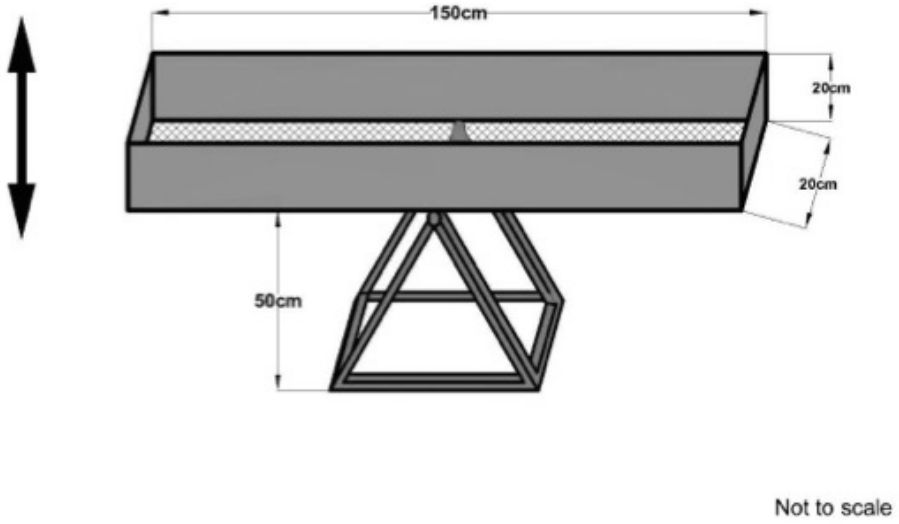

Figure 8. Configuration of the dynamic sieve stability system [20].

2.3 Influencing Mix Design Parameters and Casting Conditions

In this section, the influence of different mix design parameters and fresh properties is described. The results are mainly based on the work of El-Chabib and Nehdi [12], and Esmaeilkhanian et al. [11] [18] [21].

2.3.1 Effect of rheology

As explained in section 1.2, the rheological properties of concrete are defined by the yield stress, which is the resistance to start flow, and the plastic viscosity, which is the resistance to accelerate the material. In the following sections, one of the mix design parameters is varied to investigate dynamic segregation. With each variation, the rheological properties are also influenced. Based on the measurements of Esmaeilkhanian et al. [21], using the tilting box described in section 2.2.6, more dynamic segregation is observed when yield stress and plastic viscosity are relatively low. Increasing the yield stress or the plastic viscosity enhance segregation resistance, all other parameters remaining the same (Figure 9). Based on measurements with the ConTec Viscometer 5 (see section 3.3.6), adequate dynamic segregation is obtained when the plastic viscosity is larger than 55 Pa s. In case the yield stress is larger than 20 Pa, the requirement on the viscosity can be lowered to 40 Pa s. As can be seen, yield stress and plastic viscosity have a synergetic effect in stabilizing concrete. This will be further discussed in section 3.4.2.

2.3.2 Effect of w/cm

El-Chabib and Nehdi [12], using the compartmented cylinder described in section 2.2.5, have determined dynamic segregation of SCC mixtures by placing the measuring cylinder under the V-Funnel apparatus. When increasing the w/cm from 0.4 to 0.58, an increase in dynamic segregation was observed [12]. This can be related to the reduction in yield stress and plastic viscosity when adding water to the mixture [22].

2.3.3 Effect of chemical admixtures

Superplasticizers (SP) are known to mainly reduce the yield stress in concrete [22]. Viscosity-modifying agents (VMA) have the tendency to increase both yield stress and plastic viscosity [22], dependent on the type of VMA. Based on the results on rheology, increasing the dosage of SP should lead to an increase in dynamic segregation, while increasing the amount of VMA should have the opposite effect. The results from

El-Chabib and Nehdi [12] confirm this statement. Furthermore, the results in Figure 9 were mainly obtained by varying w/cm and admixture contents [11] [21].

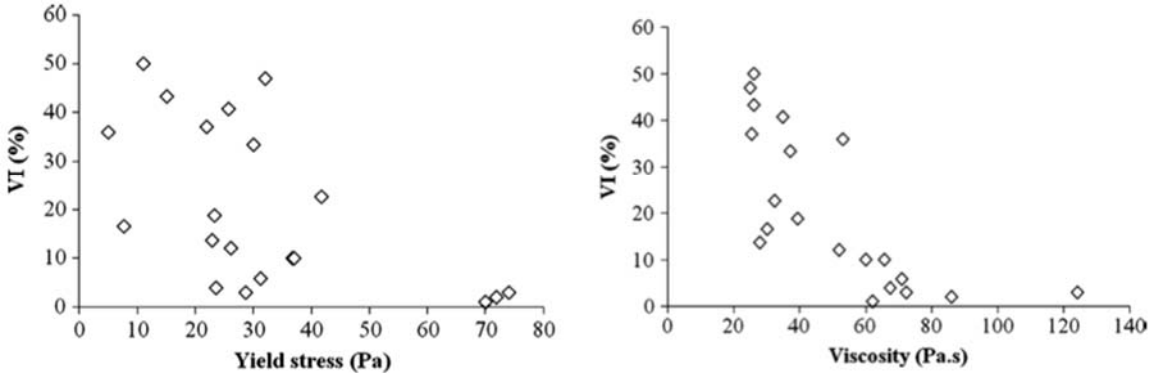

Figure 9. Influence of rheological properties (yield stress left and plastic viscosity right) on the volumetric index in the T-box, describing dynamic segregation [11].

2.3.4 Effect of paste volume

Increasing the paste volume decreases the yield stress and plastic viscosity, as the overall amount of water increases. Esmaeilkhanian et al. [11] and El-Chabib and Nehdi [12] have investigated the influence of the paste volume on dynamic segregation of concrete. El-Chabib and Nehdi have varied the amount of cementitious materials from 375 to 530 kg/m^3 (630 to 900 lbs/yd^3), while keeping the w/cm constant at 0.40 and 0.45. For w/cm = 0.45, an increase in paste volume increases dynamic segregation, which is represented by the solid line in Figure 10. However, decreasing the w/cm to 0.40 results in a negligible effect of the paste volume (Figure 11). It is suspected that for the w/cm = 0.40, the rheological properties are sufficiently high to restrict dynamic segregation, while for the w/cm = 0.45, a significant reduction in rheological properties could be obtained when increasing paste volume.

Esmaeilkhanian [11] has studied the influence of the paste volume by increasing all constituents of the paste proportionally, including SP and VMA contents. Although the concrete was statically unstable at high paste volumes, rendering the results in the T-box invalid, an increase in dynamic segregation was observed with increasing paste volume. In fact, dynamic segregation is controlled by the rheology of the cement-paste or the mortar (dependent on the approach), while the study of Esmaeilkhanian [11] used concrete rheology. As a result, it can be doubted whether concrete rheology is sufficient to explain the observed effects on dynamic segregation, or whether the paste volume has an additional effect. This is discussed in section 3.4.5.

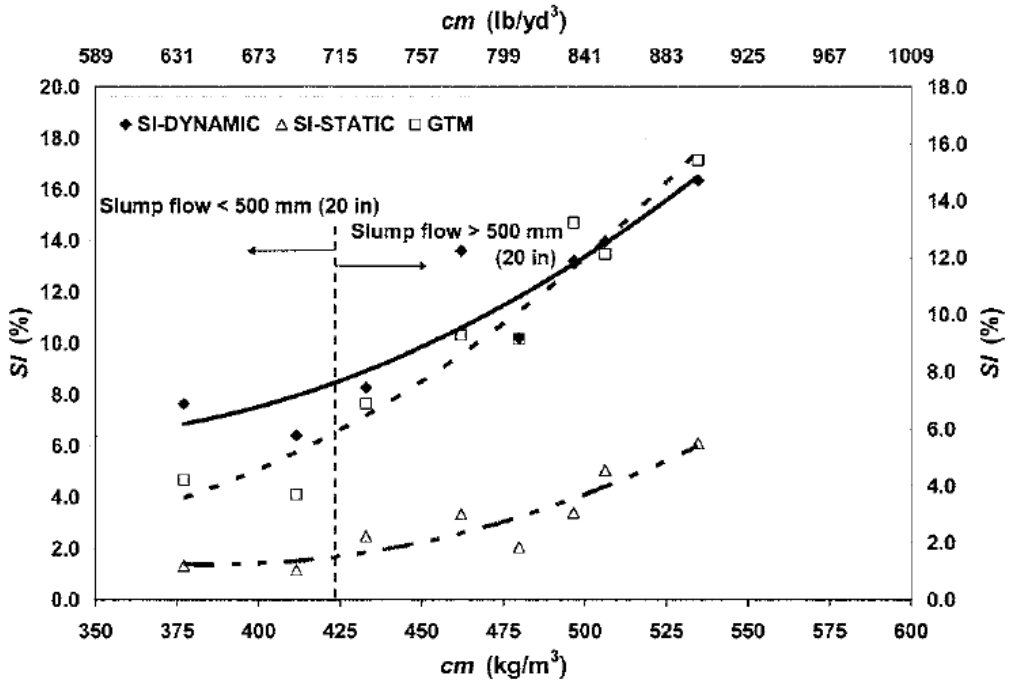

Figure 10. Effect of the amount of cementitious materials (and thus paste volume) on the dynamic segregation of SCC (solid line), at w/cm = 0.45 [12].

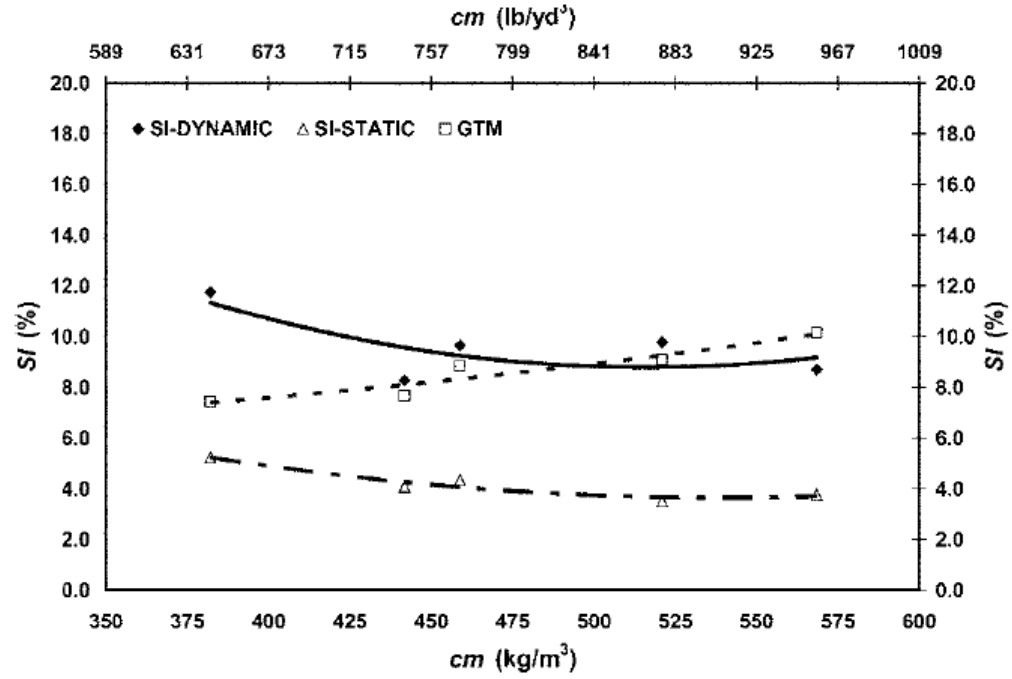

Figure 11. Effect of the amount of cementitious materials (and thus paste volume) on the dynamic segregation of SCC (solid line), at w/cm = 0.40 [12].

2.3.5 *Effect of sand-to-total aggregate ratio (S/A)*

Modifying the content of sand relative to all aggregates also influences dynamic segregation. El-Chabib and Nehdi [12] have investigated the influence of coarse aggregate-to-total aggregate ratio (CA/A) (which is 1 – S/A) on dynamic segregation of SCC. Figure 12 shows that an optimum CA/A, and thus an optimum S/A, exists to limit dynamic segregation.

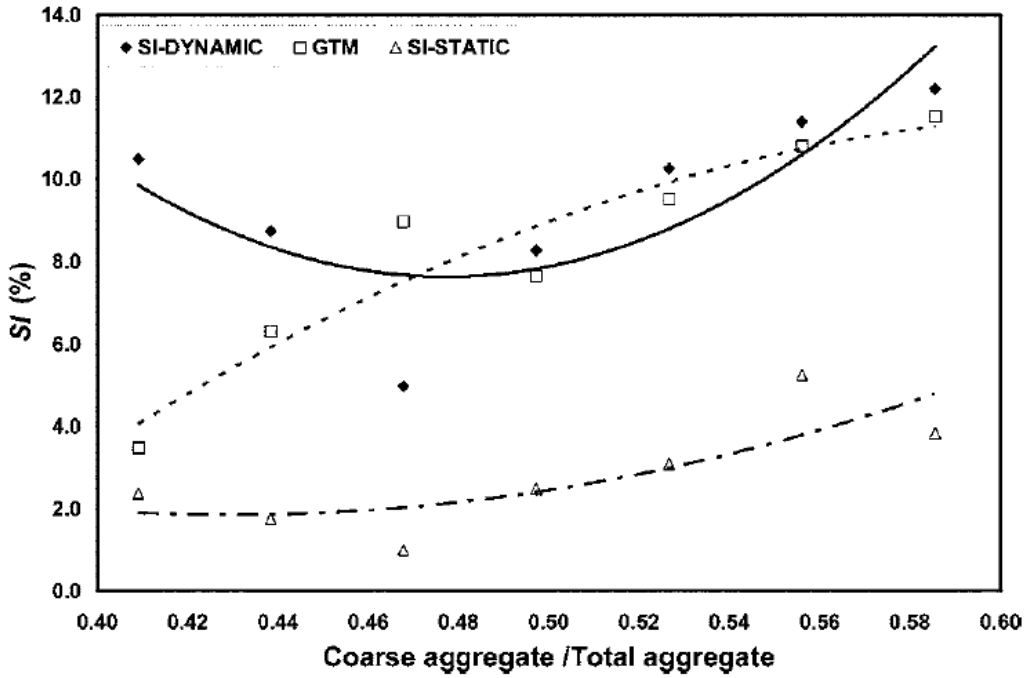

Figure 12. Influence of coarse aggregate-to-total aggregate ratio on dynamic segregation (solid line). [12].

2.3.6 *Effect of the maximum aggregate size*

Esmaeilkhanian [11] has investigated the effect of the maximum aggregate size on dynamic segregation, and has concluded that increasing the size of the aggregates increases dynamic segregation. This observation is in agreement with the results on static segregation, as gravity is proportional to the volume of the particle (r^3), while stabilizing effects, caused by the yield stress or the viscosity, are related to the surface area of the aggregate (r^2). As a result, increasing the radius of the particle increases its potential to segregate. Furthermore, any recommendations made to control segregation based on rheology or workability should be as a function of the maximum aggregate size, and potentially the grain size distribution employed.

2.3.7 *Effect of flow distance*

The advantage of the tilting box test [11] [18] is that the cycling motion allows to simulate different flow distances. Theoretical calculations reveal that each 30 cycles would correspond to 2.25 m (7.4 ft) of flow distance. Increasing the flow distance increases dynamic segregation. However, the rate of increase in dynamic segregation decreases with increasing number of cycles. This means that initially, a lot of segregation will happen, but the further the concrete flows, segregation will increase, but at a slower pace.

2.3.8 *Effect of flow velocity*

A second advantage of the tilting box test is the control of the cycle time. Varying the cycle time changes the flow velocity and influences dynamic segregation. Esmaeilkhanian et al. [11] [18] and Spangenberg et al. [23] report that dynamic segregation generally decreases with increased flow speed. This can be attributed to

the increased drag exerted on the coarse aggregates when increasing flow velocity. However, decreasing the velocity beyond a critical point (which appeared a 4 s cycle time according to [11] [18]), leads to a decrease in dynamic segregation. It was argued that with decreasing flow velocity, the shear rate decreases. This leads to a lower volume of concrete which is effectively sheared, while a large portion flows as a pure plug. In case of plug flow, the segregation can be regarded as purely static, not as dynamic.

2.3.9 Effect of formwork dimensions

Daczko [24] has investigated the influence of formwork dimensions on dynamic segregation and has concluded that narrower formworks increase dynamic segregation. However, in this work, the opposite has been observed, which is described in section 3.4.7.

3 Influence of Mix Design Parameters on Dynamic Segregation of SCC

In this section, the laboratory work to determine the most influential mix design factors for dynamic segregation is discussed.

3.1 Work Plan

To study the influence of mix design parameters on dynamic segregation, the work has been divided into three subtasks, reflecting modifications relative to the reference mixture.

- Subtask 1: Standard VMA-type SCC mix design based on previous experiences of the research group. Modifications in admixture contents (SP and VMA).
- Subtask 2: Coreslab Structures reference mix design, made with the materials available at Missouri S&T. Modifications in w/cm, paste volume, S/A and SP content.
- Subtask 3: Coreslab Structures reference mix design, made with materials shipped from Coreslab Structures in Marshall, MO. Modifications in SP/VMA content, air-entraining agent (AEA) and S/A.

As a result, the materials used in each subtask are different, which is explained in the next section. This is followed by the presentation of the test methods and the discussion of the results.

3.2 Concrete Mix Designs

3.2.1 Materials

3.2.1.1 Cement and supplementary cementitious materials

In subtasks 1 and 2, an ordinary Type I/II Portland cement from a producer in Missouri was used. For subtask 3, the cement was a Type III rapid hardening cement employed at Coreslab Structures. The relative densities of the cements are 3.11 and 3.15, respectively. A commercially available Class F fly ash, with relative density of 2.38 was used as a partial replacement of the cement in subtask 1.

3.2.1.2 Fine aggregates

Two types of sand were used during this laboratory stage. Missouri river sand (MR) was employed for subtasks 1 and 2, while Kansas River sand (KR) was selected for subtask 3. Both sands have similar relative densities of 2.61 or 2.62 and an absorption of 0.4%. The Missouri river sand had a fineness modulus of 2.72, while this value was 2.53 for the Kansas river sand. The grain size distribution of both sands are mostly within the limits of ASTM C33/C33M-16 (Figure 13) [25].

3.2.1.3 Coarse aggregates

Four different coarse aggregates were employed: three crushed limestones and one pea gravel. Crushed limestone 1 (CL 1) had a nominal maximum aggregate size of 9.5 mm (3/8”), a relative density of 2.55 and an absorption of 3.6%. For the pea gravel, these values were 4.75 mm (#4), 2.40 and 3.6%, respectively. CL 1 was employed as sole coarse aggregate in subtask 1, while it was combined with the pea gravel in subtask 2. Crushed limestones 2 and 3 (CL 2, CL 3) were coarse aggregates shipped from Coreslab Structures. Their nominal maximum aggregate sizes were 12.5 mm (1/2”) and 9.5 mm (3/8”), respectively. The relative density of both coarse aggregates was 2.67 and the absorption was 1.4% and 1.6% for CL 2 and CL 3, respectively. The grain size distributions of the coarse aggregates are depicted in Figure 14.

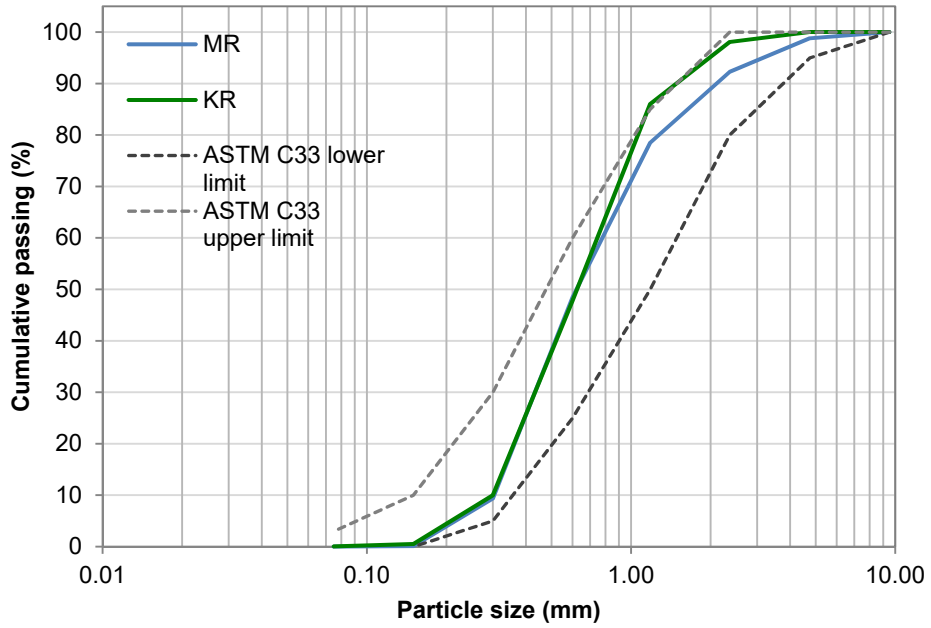

Figure 13. Grain size distribution of the Missouri river (MR) and Kansas river (KR) sand.

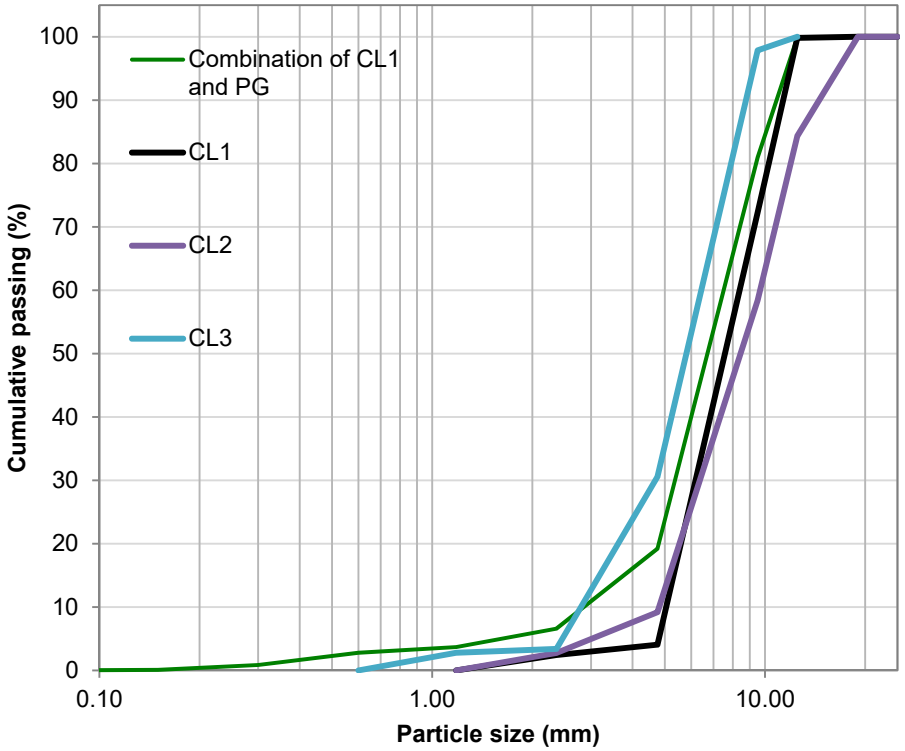

Figure 14. Grain size distribution for the crushed limestones (CL 1, CL 2 and CL 3), and the combination of CL 1 with the pea gravel.

3.2.1.4 Chemical admixtures

For subtasks 1 and 2, the superplasticizer (SP) employed was polycarboxyl-ether based and is well known for its long workability retention. The long workability retention was desirable for the research team to extend testing time. The viscosity-modifying agent (VMA) is welan-gum based and compatible with the SP. No air-entraining agents were incorporated in the mixtures in subtasks 1 and 2. For subtask 3, the commercial chemical admixture was a product combining SP and VMA, showing short workability retention, typical for the precast industry. In order to imitate as well as possible the mixture from Coreslab Structures, a commercially available air-entraining agent (AEA) was also used.

3.2.2 Mixing procedure

For subtasks 1 and 2, all mixtures were prepared in 100 L (3.5 ft^3) batches, in a drum mixer with 150 L (5.3 ft^3) capacity. After correcting for the moisture content of the sand, the coarse aggregate, sand and half of the mixing water were introduced into the mixer and mixed for 30 s. This was followed by the introduction of all cement and fly ash, if applicable, with the remaining part of the water. Mixing continued for 1 minute after which the chemical admixtures were added. Mixing was resumed for 2 minutes, followed by a 3 min rest period and another 2 min of mixing. After mixing, the consistency of the concrete was evaluated visually or by means of slump flow to assure the mixture was in the appropriate range. If the slump flow was too low, an additional quantity of SP was added.

For subtask 3, the same procedure was followed, but the mixing was performed in an intensive shear mixer to simulate the mixing operations at a precast plant. For all mixtures, except when the admixture content was varied deliberately to modify the slump flow, the target slump flow was 700 ± 20 mm (28.3 ± 0.8 in.).

3.2.3 Mix designs

3.2.3.1 Subtask 1

The reference mix design in subtask 1 was a VMA-type SCC mix design employed by the research team for other projects. It was produced with Type I/II cement, Class F fly ash, MR sand and CL 1. The chemical admixtures were the superplasticizer with long workability retention and the compatible VMA. No air-entraining agent was used. The mix designs are displayed in Table 1a (metric) and Table 1b (English units). Paste volume, w/cm and sand-to-total aggregate ratio are also included in Table 1a.

Table 1a. Mix designs for subtask 1 (in kg/m^3).

Material	Reference	- SP	+ SP	No VMA	+ VMA
Water	191	191	191	191	191
Cement	384	384	384	384	384
Fly ash	96	96	96	96	96
SP	2.08	1.66	2.41	2.08	2.08
VMA	0.24	0.24	0.24	0	0.60
Coarse Aggregate	710	710	710	710	710
Fine aggregate	888	888	888	888	888
Paste volume (%)	38	38	38	38	38
w/cm	0.40	0.40	0.40	0.40	0.40
S/A	0.56	0.56	0.56	0.56	0.56

Table 1b. Mix designs for subtask 2 (in lb/yd^3).

Material	Reference	- SP	+ SP	No VMA	+ VMA
Water	321	321	321	321	321
Cement	647	647	647	647	647
Fly ash	162	162	162	162	162
SP	3.51	2.80	4.06	3.51	3.51
VMA	0.40	0.40	0.40	0	1.01
Coarse Aggregate	1196	1196	1196	1196	1196
Fine aggregate	1497	1497	1497	1497	1497

3.2.3.2 Subtask 2

The SCC mix design for subtask 2 was based on a typical Coreslab Structures SCC mix design. For proprietary reasons, the mix design cannot be revealed. The materials used were a Type I/II cement, MR sand, CL 1 combined with the pea gravel and the long workability retention SP with the compatible VMA. No air-entraining agents were used in this subtask, although a lot of air has been observed. The following modifications were performed, relative to the reference mix design:

- The w/c was changed ± 0.05 to 0.35 and 0.45.
- The paste volume was varied with 25 l/m^3, or 2.5% of the concrete volume
- The sand-to-total aggregate ratio was altered by ± 0.05, from 0.51 (ref) to 0.46 and 0.56.
- The total amount of SP was modified to increase or decrease the slump flow.

Key properties of the mix designs are displayed in Table 2.

Table 2. Mix design properties for subtask 2

	Reference	Ref 2	- w/cm	+ w/cm	- paste	+ paste	- s/a	+ s/a	- SP	+ SP
Paste volume (%)	39.5	39.5	37	42	37	42	39.5	39.5	39.5	39.5
w/cm	0.40	0.40	0.34	0.45	0.40	0.40	0.40	0.40	0.40	0.40
S/A	0.51	0.51	0.51	0.51	0.51	0.51	0.46	0.56	0.51	0.51

3.2.3.3 Subtask 3

In subtask 3, variations were made relative to the reference mixture, made with Coreslab Structures materials. For this subtask, a Type III cement, KR sand, CL 2 and 3 were used. The chemical admixture was the combined SP/VMA with short workability retention, and an air-entraining agent was employed. In this subtask, the following parameters were varied:

- The SP dosage was varied to modify the slump flow
- The content of the AEA was halved and doubled to investigate the effect of air.
- The S/A was changed with ± 0.05 compared to the reference.

Table 3 shows key properties of the mixtures tested in subtask 3.

Table 3. Key mix design properties for subtask 3

Material	Reference	Ref 2	- SP	+ SP	- AEA	+ AEA	- s/a	+ s/a
Paste volume (%)	38	38	38	38	38	38	38	38
w/cm	0.36	0.36	0.36	0.36	0.36	0.36	0.36	0.36
S/A	0.51	0.51	0.51	0.51	0.51	0.51	0.46	0.56

3.3 Testing Procedure

After the slump flow of the concrete was deemed adequate, and the visual stability index was 0 or 1, indicating no static segregation, the following tests were performed. A detailed description of the tests is given in the following sections:

- Slump flow and T50
- V-Funnel flow time
- Density and air content measurement
- Sieve stability test, measuring static segregation
- Tilting box test, measuring dynamic segregation
- Concrete rheology with the ConTec Viscometer 5

3.3.1 Slump Flow and T50 (ASTM C1611)

Concrete was put in the Abrahm's cone, placed on the base plate. The mold is quickly removed and the final spread was measured as the average of two diameters. This test was mainly used to measure yield stress [26], but from visual examination, it was also determined if the concrete was segregating [27]. The viscosity is measured during this test by measuring the time it took takes for the concrete to flow 500 mm (25"), which is the definition of T50. None of the concrete tested in this experiment segregated during the slump flow test and no halos were seen.

3.3.2 V-Funnel flow time

The V-Funnel test is performed to measure the viscosity of concrete. The concrete is loaded into a V-shaped container. After filling, the bottom valve is opened and the time it takes for the concrete to flow through the funnel is measured. The faster the concrete flows through the funnel, the less viscous it is. The V-Funnel is depicted in Figure 15.

3.3.3 Density and air content (ASTM C 231)

Freshly mixed concrete was placed, without external consolidation, in a measuring bowl with known volume. The weight of the concrete in the bowl was determined. The bowl was covered tight with the air meter. The air content is the difference between the water level readings at the desired pressure once it was released. An aggregate correction factor was also used as per standard by taking the volume of the bowl and by knowing the original masses and volume of concrete produced.

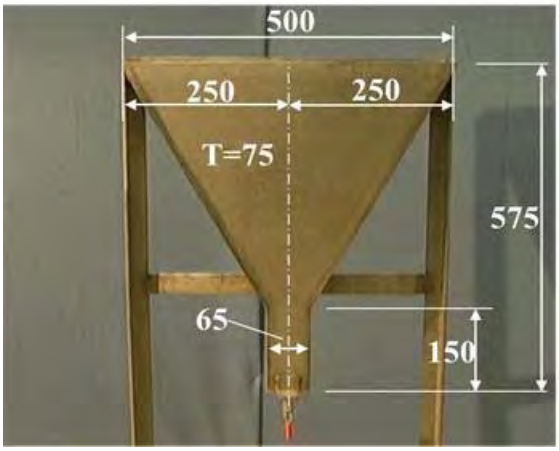

Figure 15. V-Funnel. All dimensions are in mm (25 mm = 1 inch). The width or thickness (T) is 75 mm.

3.3.4 Sieve stability (European Guidelines for SCC)

The sieve stability test is a relatively easy European test to determine static segregation of SCC [5]. This test was performed by placing 5 ± 0.2 kg (11 ± 0.44 lbs) of fresh concrete on a #4 sieve, with a pan below (Figure 16). The mass of the sample was recorded and the system was left at rest for two minutes. After this resting time, the sieve was removed and the mass of the material that percolated in the pan was obtained. The more paste that passes through the sieve to the pan, the less stable the concrete is. This is very important because the paste needs to be able to keep the aggregates suspended and guarantee homogeneity of the concrete during mixing, transport and placement. The European Guidelines for SCC [5] identified three segregation classes based on this test. A first segregation class (SR1), where segregation is less than 20% is preferred for thin slabs and vertical applications with a flow distance of less than 5 m (16.5 ft) and a confinement gap larger than 80 mm (3.15 in.). For larger flow distances, two, more severe, segregation classes are identified: SR2 and SR3, where segregation is less than 15% or 10%, respectively. In this research work, the SCC was deemed statically stable if the sieve stability test indicated 15% segregation or less.

Figure 16. Sieve stability test.

Note that the European guidelines prescribe that the concrete must be left in a bucket for 15 min prior to performing the sieve stability test. While this can enhance segregation, it can also allow the concrete to stiffen

during that time and reduce the segregation index. In this work, the waiting period was not followed and the SCC was poured on the sieve immediately after sampling.

3.3.5 Tilting box test

The tilting box test is described in section 2.2.6. The box constructed at Missouri S&T has a width of 400 mm (16 in.), which can be divided into two sections with 100 mm (4 in.) and 200 mm (8 in.) width. Both sections are filled until the concrete reaches a height of 80 mm (3.15 in.) (Figure 17). The box is tilted for 120 cycles, with a 2 s cycle duration. These parameters were selected based on the expected flow distance (9 m, 30 ft) and flow velocity. While flow distance and velocity affect the dynamic segregation of SCC (see sections 2.3.7 and 2.3.8), those parameters were not modified during this research. However, in subtask 3, and during the field work, the number of cycles was reduced to 60 to avoid the stiffening effect of the concrete to influence the results. A correction factor was applied to be able to compare the results.

The concrete is evaluated based on the volumetric index (VI) (eq. 2), determined based on the coarse aggregate contents taken in the tilt-up and tilt-down sections. Measuring dynamic segregation by means of the penetration device has been attempted, but the results appear less reliable and are hard to interpret correctly. Therefore, dynamic segregation is only assessed by the volumetric index.

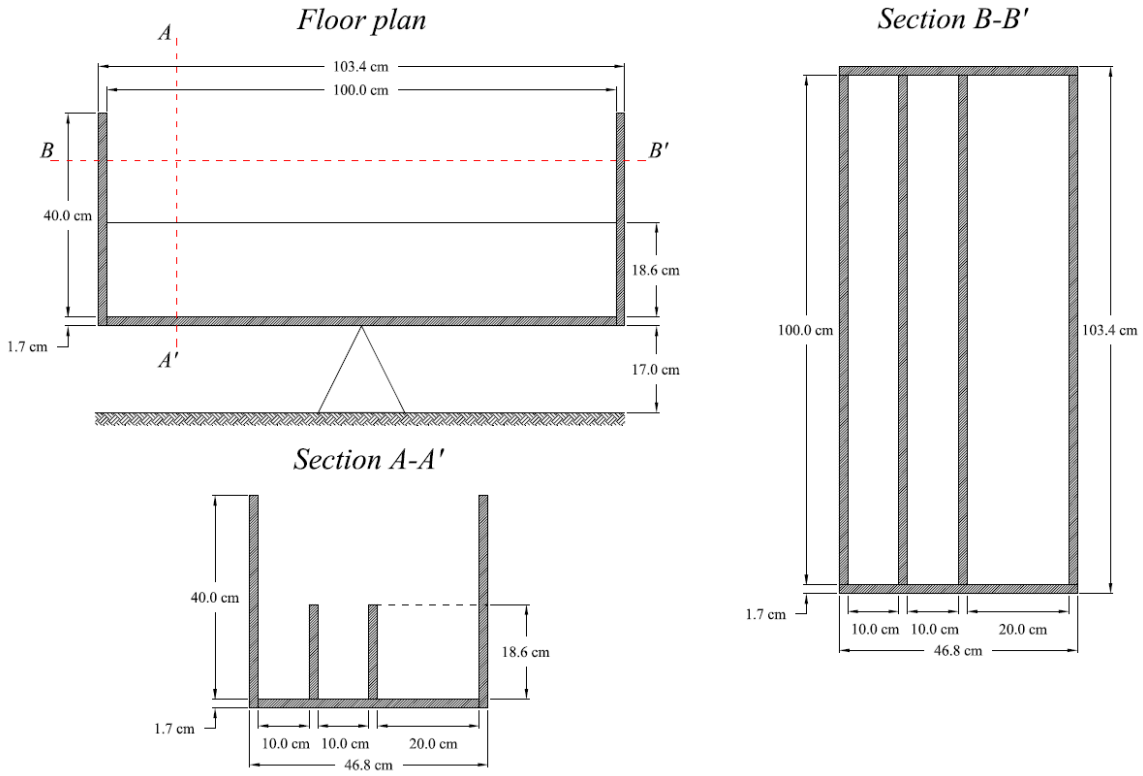

Figure 17. Configuration of the tilting box developed at Missouri S&T.

3.3.6 ConTec Viscometer 5

The rheological properties of materials are measured with rheometers, also called viscometers. For cement-based materials, due to the presence of aggregates, rheometers are typically quite large in size. The ConTec Viscometers are a series of rheometers developed for cement-based materials. They are based on the principle of the coaxial rotating cylinders, in which, in this case, the inner cylinder is stationary and the outer cylinder rotates at imposed rotational velocities [8]. The resulting torque exerted by the material is registered at the

inner cylinder. With the coaxial cylinders system, yield stress and plastic viscosity can be easily calculated from the relationship between the measured torque and imposed rotational velocity.

The ConTec Viscometer 5 is the largest of the rheometers, capable of measuring the rheological properties of concrete with a maximum aggregate size of 16 mm (5/8") (Figure 18). The bucket, which serves as outer cylinder, has a radius of 145 mm (5.71"), while the inner cylinder measures 100 mm (3.94") in radius. The height of the inner cylinder which is submerged in the concrete is measured after each test. A value of 110 mm (4.33") is aimed for. Both the inner and outer cylinders are equipped with ribs to prevent slippage between the concrete and the surfaces.

Figure 18. ConTec Viscometer 5.

During the execution of the tilting box test, the rheological properties of the concrete were determined. The materials were subjected to the highest rotational velocity during 20 s, to eliminate any effect of thixotropy on the properties [28]. The rotational velocity was decreased in 10 steps, maintaining each step during 5 seconds. In this way, the effect of dynamic segregation during the measurement is minimized. For the ConTec Viscometer 5, the maximum and minimum rotational velocity was 0.40 and 0.025 rps respectively.

At each step of the rheometer test, the average of the torque and rotational velocity was calculated, omitting the first second of the step, provided the torque value was stable with time. By means of the Reiner-Riwlin equation, the yield stress and plastic viscosity of the material can be easily derived from the relationship between torque and rotational velocity [8] [29]. In case plug flow occurred, a correction was performed [30].

3.3.7 Compressive strength testing

The compressive strength of all concrete mixtures was also determined by averaging the strength of three 100 x 200 mm (4 x 8 in.) cylinders after 28 days of curing under water, according to ASTM C39/39M-16 [31]. The specimens were cast in a single lift without consolidation. The end surfaces were grinded to assure flatness.

3.4 Results and Discussion

3.4.1 Summary of data

All data from all experiments are summarized in Table 4. The following general comments can be made about the mixtures:

- The mixture with an added SP amount for mix design 1, and the S/A = 46% mixture for mix design 3 show more than 15% sieve stability and have been excluded from further analysis.
- The most significant variations in workability and rheology were obtained by varying the w/cm.
- Mix design 1 and 2 showed relatively large air contents, despite not adding air-entraining agents
- Mix design 3 is generally stronger at 28 days, which may be due to the slightly lower w/cm and/or the use of Type III cement.

In the following sections, the specific influence of rheology, w/cm, chemical admixtures, paste volume and sand-to-total aggregate ratio on dynamic segregation in the 200 mm channel are discussed. The influence of the channel width is further analyzed by comparing the 100 mm to the 200 mm results.

Table 4. Summary of workability, dynamic segregation and compressive strength of the mixtures tested in the lab.

Mixtures		**Workability**	Slump flow (mm)	Slump flow (in.)	T 50 (s)	V-Funnel (s)	Air content (%)	Sieve stability (%)	**Dynamic segregation**	VI in 100 mm (%)	VI in 200 mm (%)	**Concrete Rheology**	Yield stress (Pa)	Plastic viscosity (Pa s)	Shear stress @ 1 s^{-1} (Pa)	**Compressive strength (MPa)**	**Compressive strength (psi)**
Mix design 1																	
Ref			710	28.0	0.6	4.2	6.5	9.8		20.3	29.9		20.7	17.5	38.2	42.1	6110
SP	+16%		760	29.9	1.6	2.8	6.8	15.5		-	-		-	-	-	-	-
	-20%		650	25.6	1.4	3.8	6.5	8.6		15.1	25.0		24.4	15.6	40.1	43.4	6290
VMA	+2.5x		670	26.4	1.4	3.5	4.3	9.9		10.7	21.6		30.2	13.3	43.5	40.8	5920
	0		700	27.6	1.1	3.5	5.5	10.0		25.9	34.2		22.3	13.6	35.9	42.7	6190
Mix design 2																	
Ref			720	28.3	1.5	3.4	6.5	7.0		13.6	21.9		10.1	12.1	22.1	45.5	6600
w/cm	0.35		690	27.2	1.3	11.0	6.5	4.8		1.3	5.4		7.5	33.5	41.0	65.2	9460
	0.45		690	27.2	1.1	2.3	2.0	8.9		7.3	17.6		21.0	9.5	30.5	50.6	7340
SP	-10%		658	25.9	0.9	3.8	6.0	7.0		4.4	13.5		14.9	15.4	30.3	50.4	7310
	+10%		740	29.1	0.9	3.1	4.5	10.7		12.6	23.2		9.6	12.3	21.8	46.6	6760
Paste	-25 l/m3		690	27.2	0.8	4.5	7.0	6.2		9.4	13.8		18.0	18.9	36.8	45.8	6640
	+25 l/m3		695	27.4	0.9	4.5	5.5	10.8		14.1	31.8		11.7	14.6	26.3	49.0	7110
S/A	46%		700	27.6	0.9	4.1	6.0	7.6		17.5	23.1		14.7	13.8	28.5	47.5	6890
	56%		695	27.4	0.7	3.9	6.5	7.2		23.3	44.1		14.4	17.5	31.9	43.6	6320
Mix design 3																	
Ref			683	26.9	1.7	8.6	8.5	6.5		0.0	4.2		25.2	22.5	47.7	68.5	9940
Ref 2			640	25.2	1.7	8.3	8.0	8.0		0.0	3.6		34.1	23.1	57.2	67.6	9800
SP	+4.8%		775	30.5	1.2	4.1	6.8	13.0		36.4	37.7		6.1	14.2	20.2	68.1	9880
	-1.2%		655	25.8	2.3	6.9	7.5	6.6		0.0	4.3		35.5	18.7	54.2	73.2	10620
AEA	+2.0x		685	27.0	1.3	6.4	12.0	9.6		0.0	0.0		31.7	17.2	48.9	41.7	6050
	-0.5x		695	27.4	1.0	7.4	5.0	11.4		0.0	2.4		24.1	23.3	47.4	80.6	11690
S/A	56%		700	27.6	1.5	7.9	9.5	6.4		0.0	0.0		31.1	22.0	53.2	62.8	9110
	46%		710	28.0	1.2	4.2	5.5	22.5		-	-		-	-	-	-	-

3.4.2 Influence of rheology

As mentioned by Esmaeilkhanian et al. [21], increasing either the yield stress or the plastic viscosity can have a stabilizing effect during the flow of SCC. This was illustrated in Figure 9. Considering the results in this work (all three subtasks combined), similar conclusions are obtained (Figure 19 and Figure 20):

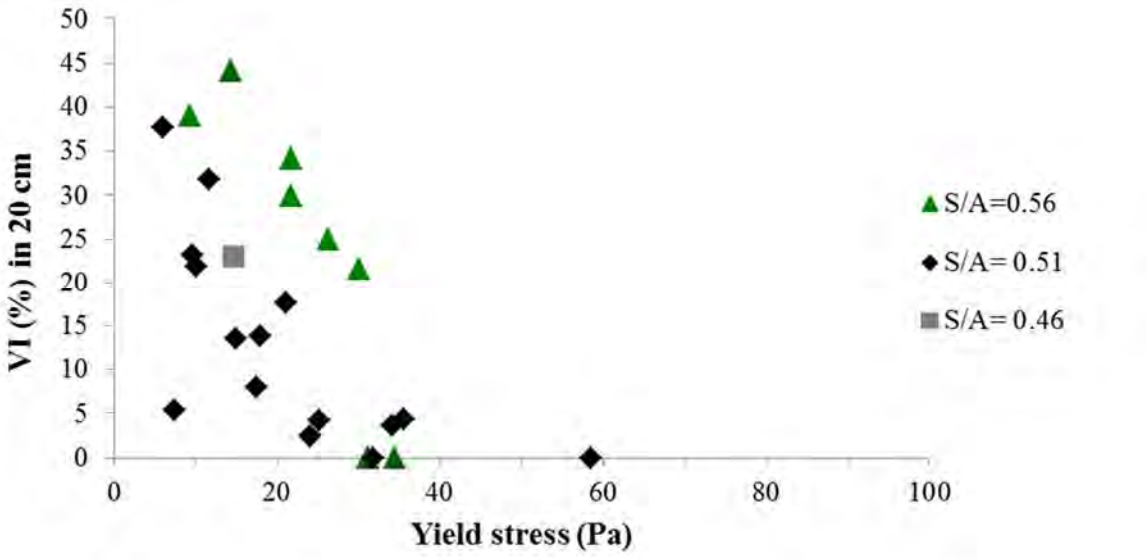

Figure 19. Increasing yield stress reduces dynamic segregation.

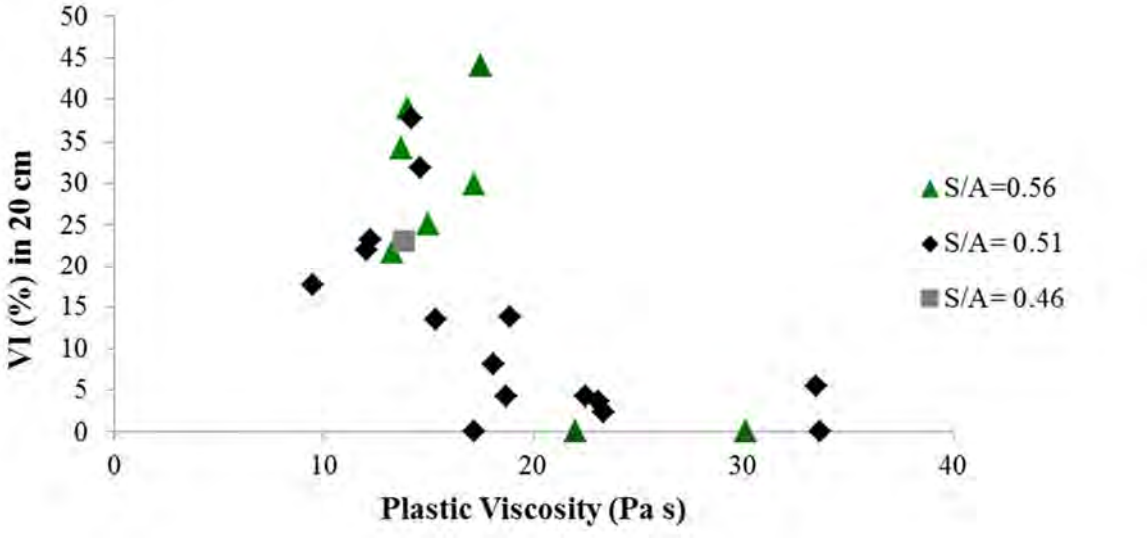

Figure 20. Increasing plastic viscosity reduces dynamic segregation.

Although yield stress and plastic viscosity have a predominant effect on dynamic segregation, formulating limiting values is not straightforward. Having a yield stress larger than 35 Pa, or a viscosity larger than 20 Pa s results in no segregation at all, but not all mixtures with values below these limits are specifically segregating. Furthermore, the sand-to-total aggregate ratio has a distinct additional effect, discussed in section 3.4.6.

When concrete flows, at least in a part of the concrete, the yield stress is exceeded. This means that the yield stress no longer contributes to the stability of the aggregates. However, the coarse aggregates are subjected

to the drag force exerted by the mortar, which carries the coarse aggregate in the flow. The larger the viscosity, and the larger the velocity, the larger the exerted drag force. In this case, the aggregate is more likely to follow the paste and will minimize its downward motion. Increasing drag force by increasing viscosity (Figure 20) or velocity (section 2.3.8 [18]) reduces the settlement of the particle until flow stops. When flow stops, the yield stress contributes to the stability, as the concrete has become static.

Increasing the yield stress, while keeping all other parameters constant, will increase the zone in the concrete which is not sheared. This zone is called the plug. In the plug, the concrete moves at uniform velocity. As the yield stress is not exceeded, it helps to keep the particle in suspension and avoids or reduces settlement. The size of the plug zone increases with increasing yield stress and decreasing velocity. This effect can hence explain the results in Figure 19 and explains why, ultimately, with decreasing velocity, dynamic segregation decreases [18], while this is opposite to the viscous drag theory.

While investigating the results, it was considered whether yield stress or plastic viscosity would play a dominant role. Therefore, a simplified calculation was made to estimate the shear stress in the tilting box with a width of 200 mm (8 in.), similar to Roussel et al. [32]. From Esmaeilkhanian [11] we know that the average flow velocity in the box is 0.25 m/s (10 in./s), the width is 200 mm (8 in.), so the shear rate is slightly larger than 1 s^{-1}. This means that the applied shear stress during flow is yield stress plus the plastic viscosity (x 1 s^{-1}), resulting in both parameters being approximately equally important. As a result, the shear stress at 1 s^{-1} has been calculated for each mixture (simply adding the values of yield stress and plastic viscosity). The results are shown in Table 4, and the influence of the shear stress at 1 s^{-1} on dynamic segregation is illustrated in Figure 21. It is clear that dynamic segregation decreases nearly linearly with increasing shear stress at 1 s^{-1}, dependent on the sand-to-total aggregate ratio (explained further).

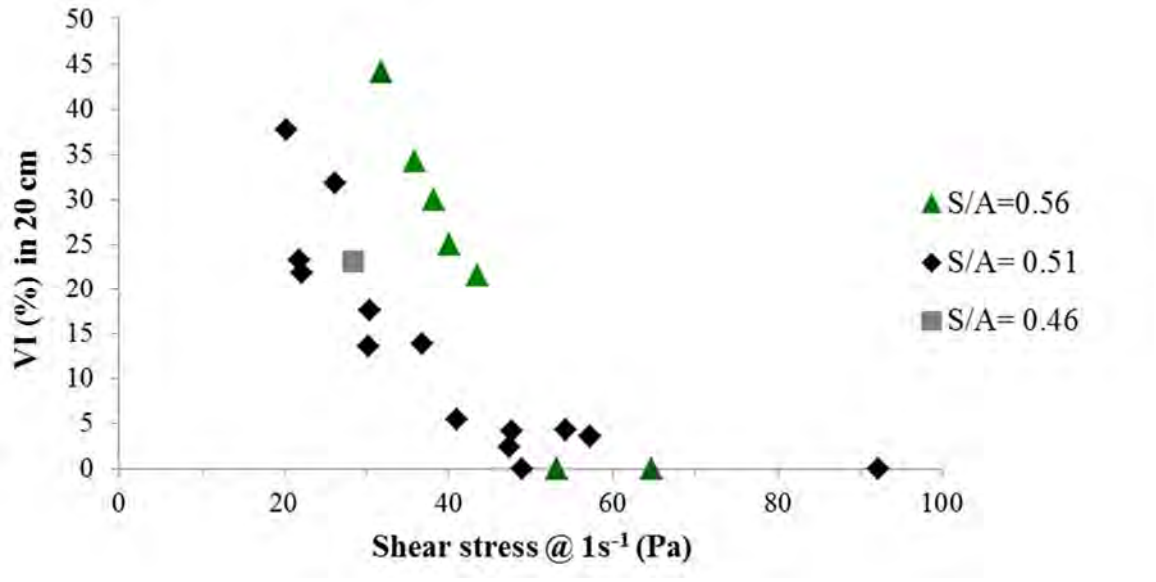

Figure 21. Dynamic segregation decreases nearly linearly with increasing shear stress at 1 s^{-1}, dependent of the S/A.

In the next sections, the influence of mix design parameters on dynamic segregation is discussed while the corresponding shear stress at 1 s^{-1} is included. It can thus be determined whether a specific factor has an influence which can be explained by means of rheology, or whether the influence is additional to the effect of rheology.

3.4.3 Influence of w/cm

For mix design 2, the w/cm was varied from 0.35 to 0.40 (ref) and 0.45, while adjusting the SP content to keep the slump flow approximately constant. Significant variations in yield stress and viscosity of the SCC mixtures are observed (Table 4). Figure 22 shows the volumetric index from the T-box (bars) and the shear stress at 1 s^{-1}. Note that the shear stress axis is inverted to enhance the visual assessment of the data. As can be seen, decreasing the w/cm has significantly increased the plastic viscosity (and thus the shear stress). Increasing w/cm, accompanied by a decrease in SP, has significantly increased the yield stress (and thus the shear stress). The influence of the w/cm, combined with a change in SP content, can thus be perfectly explained by means of rheology on dynamic segregation.

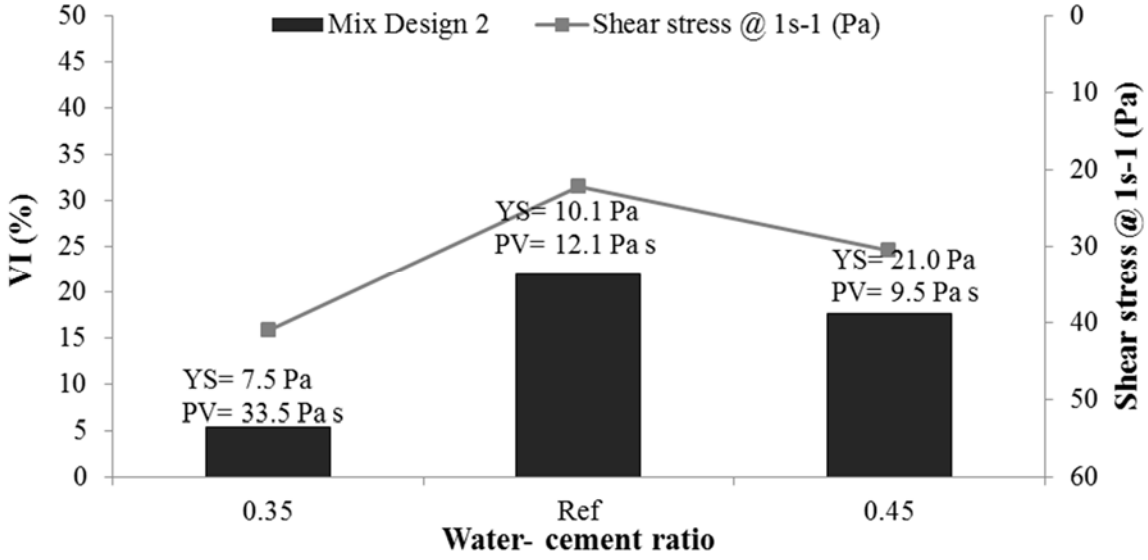

Figure 22. The influence of w/cm on dynamic segregation can be justified by means of rheology. The bars represent the VI, the line reflects the shear stress at 1 s^{-1}.

3.4.4 Influence of chemical admixtures

Three types of chemical admixtures were varied throughout the laboratory work: the SP content, in each of the subtasks, the VMA content in subtask 1, and the AEA content in subtask 3.

3.4.4.1 Superplasticizer

Modifying the SP content mostly affects the yield stress of SCC, while a minor effect on the plastic viscosity cannot be excluded [22]. As can be seen in Figure 23, Figure 24 and Figure 25, the induced modification in rheology is dictating the dynamic segregation. Almost no modification in rheology keeps VI approximately constant (Figure 23), while a substantial change in the shear stress at 1 s^{-1} leads to an important variation in dynamic segregation (Figure 25). It can thus be stated that the influence of changing the SP content on dynamic segregation is governed by rheology.

However, comparing the reference mixtures from mix design 1, 2 and 3 may indicate an apparent discrepancy. Reference mix design 1 shows the highest dynamic segregation, while reference mix design 2 has the lowest shear stress at 1 s^{-1}. The difference can be explained in two ways: Mix design 1 has a S/A = 0.56, while mix design 2 is made with S/A = 0.51, and it is shown in Figure 21 that the S/A has an additional effect on dynamic segregation. Secondly, for mix design 2, the coarse aggregate (CL 1) was combined with pea gravel, while only CL 1 was used for mix design 1. This could lead to an enhanced particle lattice effect in mix design 2, reducing (dynamic) segregation. The reference mixture for mix design 3 shows a

significantly higher shear stress at 1 s^{-1}, compared to mix design 2. This can be attributed to the different cement type (Type III vs. Type I/II), the chemical admixture and the slightly lower w/cm. Due to the high shear stress at 1 s^{-1} for reference mix design 3, dynamic segregation is almost negligible.

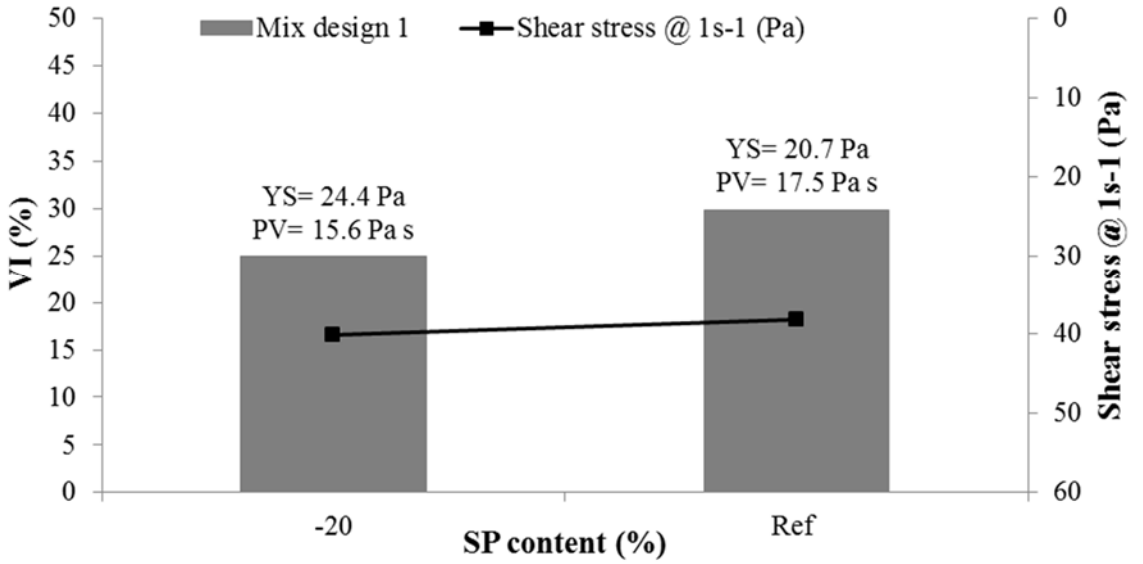

Figure 23. Decreasing SP content in mix design 1 slightly increases the shear stress at 1 s^{-1}, resulting in a decrease in dynamic segregation.

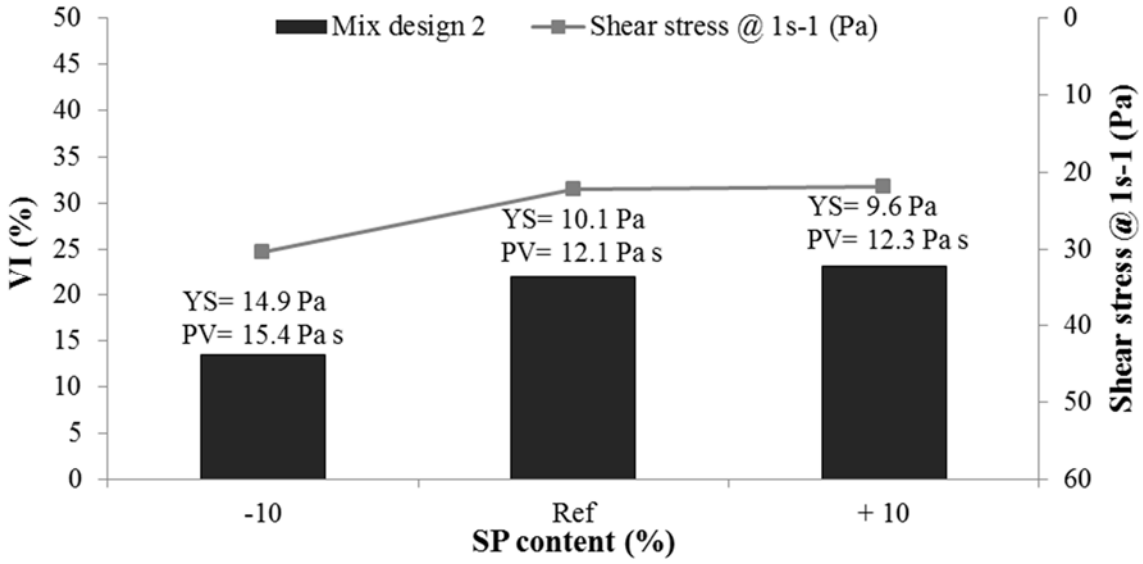

Figure 24. Modifying the SP content for mix design 2 influences dynamic segregation similarly as rheology.

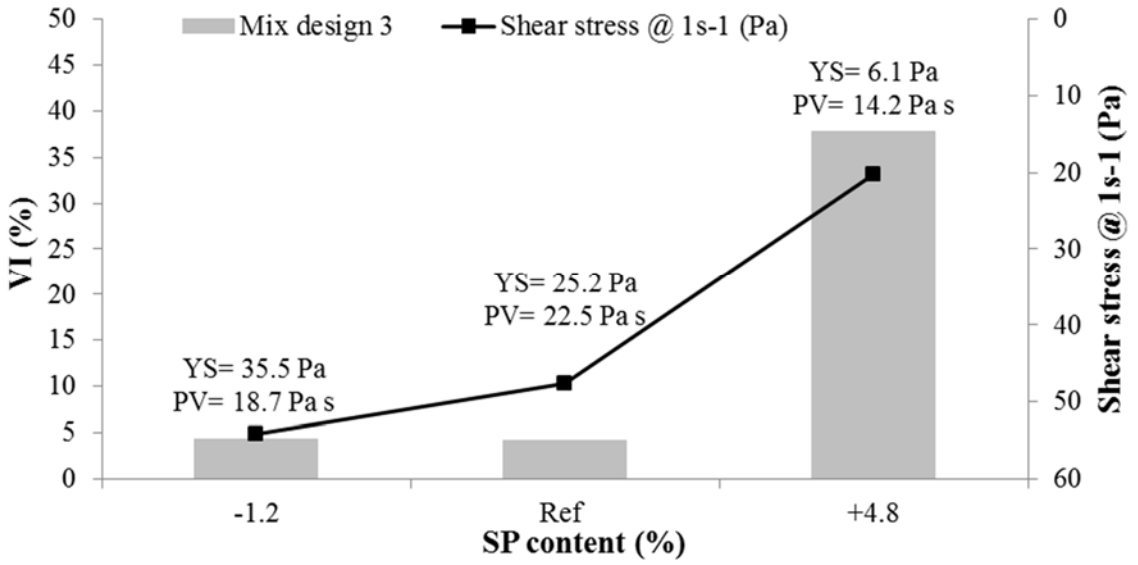

Figure 25. For mix design 3, the addition of SP has a detrimental effect on dynamic segregation, supported by the rheology results.

3.4.4.2 Viscosity-modifying agent

For mix design 1, the VMA content was varied from zero to 2.5 times the dosage in the reference mixture. Figure 26 shows a clear increase in shear stress at 1 s^{-1} with increasing VMA dosage, which is similar to the observed decrease in dynamic segregation. As a result, modifying the VMA dosage influences dynamic segregation according to the influence of rheology.

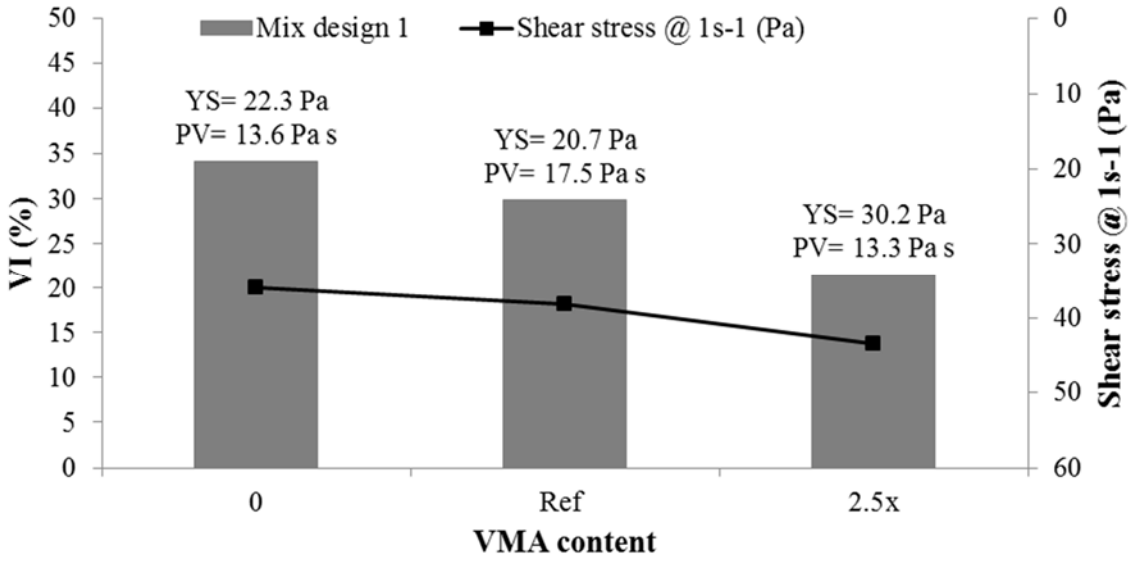

Figure 26. The influence of the VMA on dynamic segregation follows the results of rheology.

3.4.4.3 Air-entraining agent

For the air-entraining agent, which was only employed in mix design 3, the variations in rheological properties are minimal, and all results for dynamic segregation are very low. The effect of AEA on dynamic segregation is expected to be minor, unless large modifications in rheology can be induced.

3.4.5 Influence of paste volume

The paste volume was only modified for mix design 2 with ± 2.5% paste per unit volume of concrete (25 l/m^3). The SP dosage was adjusted to ensure an approximately constant slump flow. Figure 27 shows that dynamic segregation increases with increasing paste volume. However, the shear stress at 1 s^{-1} trend is not in agreement with the VI, especially when increasing the paste volume. Increasing paste volume decreases the amount of coarse aggregates (proportionally to the sand), which creates more space for the coarse aggregates to move into. Furthermore, it would have been more correct to express dynamic segregation as a function of mortar rheology (which was unsuccessfully attempted due to sampling problems).

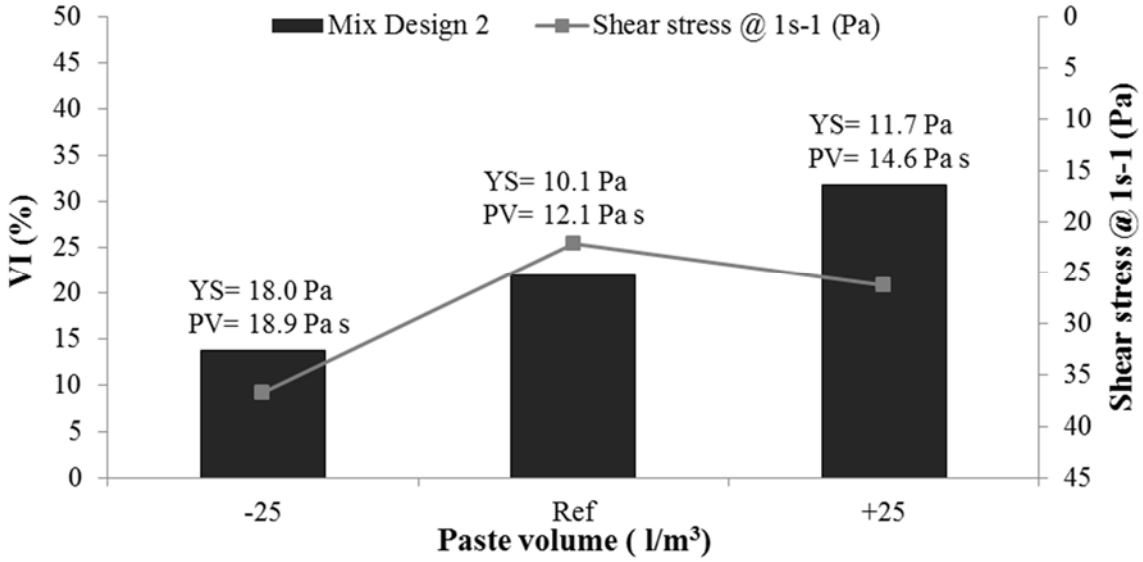

Figure 27. When modifying the paste volume, the VI does not entirely follow the influence of rheology.

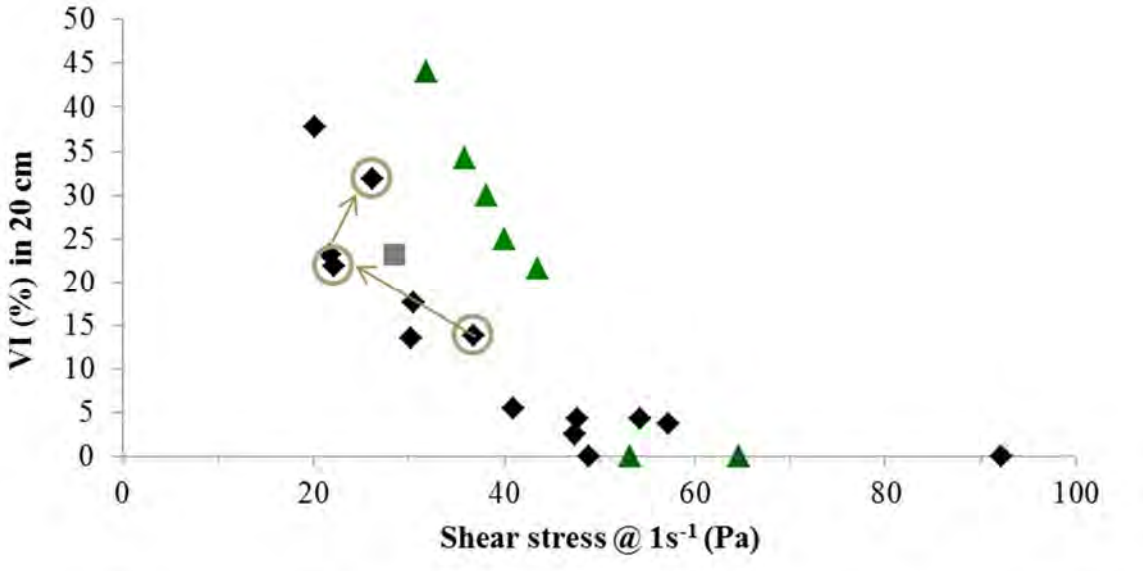

Figure 28. Reproduction of Figure 21, indicating where precisely the points with different paste volume are located. They do not necessarily follow the linear trend.

Figure 28 is a reproduction of Figure 21, in which the points with different paste volumes are highlighted. The arrows indicate the increase in paste volume from 37% over 39.5% to 42% (including air). It can be clearly seen that when increasing the paste volume up to 42%, the trend is no longer followed. Hence, modifying the paste volume has an additional influence on dynamic segregation, compared to the influence of concrete rheology.

3.4.6 Influence of sand-to-total aggregate ratio (S/A)

It was already indicated in Figure 21 that increasing S/A from 0.51 to 0.56 significantly alters the VI – shear stress at 1 s^{-1} relationship. Figure 29 confirms this statement. In fact, it appears even that S/A dominates the effect of rheology, as the VI and shear stress results do not agree at all. Increasing S/A has a similar effect as increasing the paste volume: less coarse aggregates are present, and they have more room to move without interacting with other coarse aggregates. However, this theory does not explain the influence of a decrease in S/A, as dynamic segregation should be reduced. This could, although no certainty exists, be explained by the reduced particle lattice effect, making it easier for coarse aggregates to sink, as their movement is not inhibited, or slowed down, by the movement of smaller particles.

However, it should be noted that the results shown in Figure 29, obtained for mix design 2, are not applicable on mix design 3. Table 4 shows that increasing S/A from 0.51 to 0.56 does not provoke additional dynamic segregation for mix design 3. It should however be noted that, even for the reference mix design 3, the shear stress at 1 s^{-1} was already elevated and the mixture showed almost no dynamic segregation. Increasing S/A to 0.56 had no destabilizing effect, probably because the rheology was sufficient to prevent dynamic segregation. However, decreasing S/A to 0.46 for mix design 3 had a significant destabilizing effect, as the sieve stability (static segregation) was significantly higher. The differences between mix design 2 and 3 may also be explained by the different sources of the sand and coarse aggregates, which may shift the optimum S/A for stability.

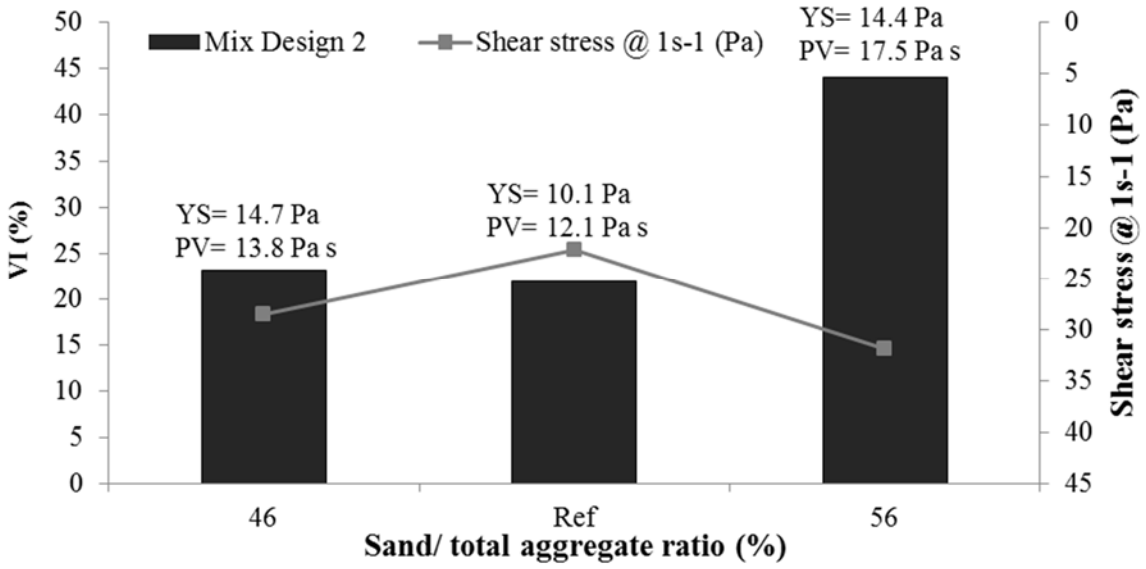

Figure 29. S/A influences dynamic segregation in a different way than rheology.

3.4.7 Influence of channel width

In Figure 30, all results obtained in the narrow channel with 100 mm (4 in.) width are plotted as a function of the VI values obtained in the 200 mm (8 in.) counterpart. It can be observed that dynamic segregation is lower in the narrow channel: it is reduced by approximately 35%. This effect can be attributed to two phenomena: as the average velocity is assumed to be the same in both channels, the peak velocity is higher

in the narrow channel. As explained when discussing viscous drag: higher velocity induces less segregation. Secondly, as the channel is narrower, the wall effect may become more important, slightly increasing the amount of coarse aggregates in the effective flow domain, leaving less space for them to segregate. Which theory is most applicable still needs to be investigated.

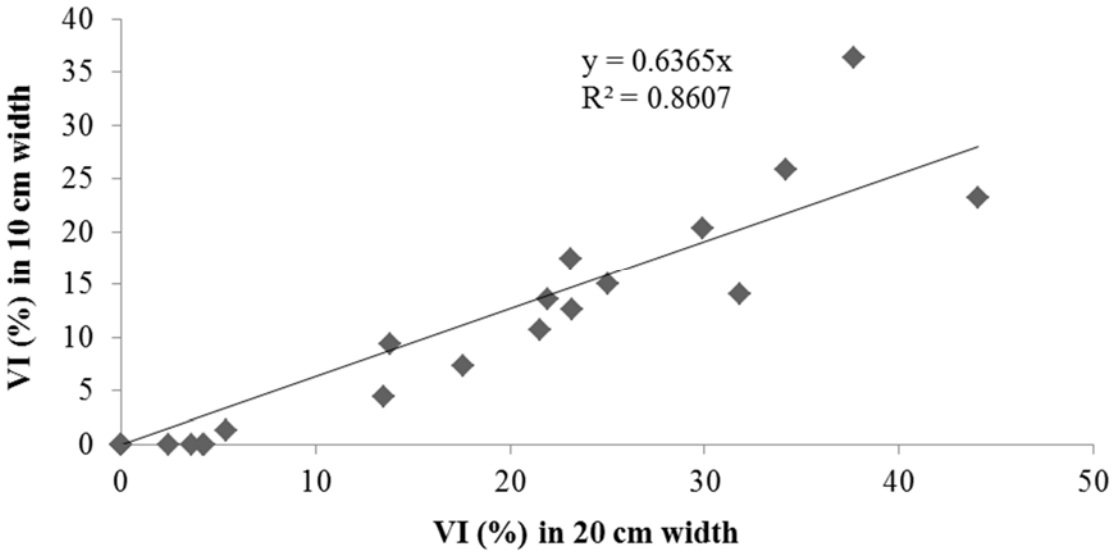

Figure 30. The dynamic segregation in the narrow channel (100 mm, 4 in.) appears approximately 35% lower than in the standard channel (200 mm, 8 in.)

3.5 Summary

Twenty two different SCC mix designs were evaluated for dynamic segregation. Three different baseline mixtures were prepared, based on the source of the mix design (S&T or Coreslab Structures) and the materials (available at S&T or shipped from Coreslab Structures). The mix designs were modified for SP content, VMA content, AEA content, w/cm, paste volume and sand-to-total aggregate ratio. The following conclusions can be drawn from the laboratory investigation:

- Both yield stress and plastic viscosity of concrete have a stabilizing effect. Increasing either decreases dynamic segregation.
- There exists a quasi-linear relationship between the shear stress at 1 s^{-1} (which is obtained by adding the yield stress and the plastic viscosity x 1 s^{-1}), and dynamic segregation.
- For any modification in mix design factors on the paste level: w/cm, SP, VMA, AEA, without modifying the paste volume, the dynamic segregation obeys the observed relationship with rheology.
- Modifying paste volume has an additional effect on dynamic segregation, as an increase in paste volume reduces the amount of coarse aggregates leaving them more space to migrate.
- Decreasing S/A had a destabilizing effect, as the dynamic segregation no longer followed the trend with rheology (mix design 2), or provoked significant static segregation (mix design 3). This can be attributed to a reduced particle lattice effect.
- Increasing S/A led also to a destabilization, as the dynamic segregation increased with increased shear stress at 1 s^{-1} (opposite to the rheology trend). This was observed for mix design 2 by explicitly increasing S/A, and by comparing mix design 1 (S/A = 0.56) and 2 (S/A = 0.51), with similar

rheology. However, for mix design 3, almost no dynamic segregation was observed for the reference due to the higher shear stress at 1 s^{-1}, and an increase in S/A did not alter the behavior.

- The optimum S/A is probably dependent on the aggregate gradation and the particle lattice effect.
- Decreasing the channel width from 200 mm (8 in.) to 100 mm (4 in.) reduced dynamic segregation by approximately 35%.
- Based on the obtained results, to avoid dynamic segregation (VI < 20% or 25%), in the 200 mm (8 in.) channel, the shear stress at 1 s^{-1} should remain larger than 30 Pa, for S/A = 0.51, and 40 Pa for S/A = 0.56. However, these recommendations are only valid for the nominal maximum aggregate sizes employed.

4 Influence of Dynamic Segregation on Homogeneity of Pre-Cast Beams

This section describes the execution and analysis of the tests performed at Coreslab Structures. In total, nine full-scale beams were cast: six rectangular and three I-beams. Three of the rectangular beams had a length of 18 m (60 ft), all other beams were 9 m (30 ft) long. The variations in mix design, fresh properties (including dynamic segregation), compressive strength on approximately 150 cores, ultrasonic pulse velocity results on the same cores, and directly applied on three of the beams, and the bond strength of prestress strands with the concrete are described.

4.1 Work Plan

To study the influence of dynamic segregation on the homogeneity of pre-cast beams, the following series of tests were executed:

- Casting of beams in two fases: Beams 1 to 8 in August 2015, Beam 9 in February 2016. In parallel to placing SCC in the beams, the fresh concrete was characterized.
- Determination of the ultrasonic pulse velocity (UPV) directly measured on beams 1, 2 and 5, by the research team of Dr. J.A. Hartell of Oklahoma State University
- Determination of the bond strength of vertically embedded strands
- Coring of specimens to determine UPV on the cores, compressive strength, and aggregate content, sorptivity and air void distribution (the latter results will be available in an addendum).

4.2 Concrete Mix Designs

4.2.1 Materials

The materials used for the production of the beams are a Type III cement, Kansas River sand, crushed limestone (CL 2 and 3), the combined HRWRA –VMA and AEA, also used in subtask 3 of the laboratory study. More detailed information on the materials can be found in sections 3.2.1.1 to 3.2.1.4.

4.2.2 Concrete mix designs

The first beam was cast with a reference SCC, typically used at Coreslab Structures in Marshall, MO. For the following beams, the research team has imposed some changes to alter the dynamic segregation of the beams: changing w/c, paste volume, S/A, and admixture contents. For proprietary reasons, the mix designs cannot be displayed, but Table 5 shows the details of the changes.

Table 5. Key properties of Mix designs employed at Coreslab Structures.

	Beam 1	Beam 2	Beam 3	Beam 4	Beam 5	Beam 6	Beam 7	Beam 8	Beam 9
w/c	0.36	0.39	0.39	0.44	0.36	0.36	0.36	0.36	0.36
S/A	0.51	0.51	0.51	0.51	0.56	0.51	0.51	0.56	0.56
Mod	Ref	w/c	Paste volume	w/c	S/A	Ref	Paste volume	S/A	S/A

4.3 Testing Program

Tests were executed on the concrete during casting, and on the hardened beams. This section describes in detail how the tests were performed.

4.3.1 Concrete beams

In total, nine beams were produced, of which six were rectangular, and three were MoDOT approved I-shaped beams. Beams 2, 4 and 9 were 18 m long (60 ft), all others were 9 m long (30 ft). The rectangular beams had a width of 457.2 mm (18 in), and 915 mm high (36 in). Six 12.5 mm prestress strands were installed at the bottom, and two at the top. Minimum shear reinforcement was installed in the beam, using #4 steel bars. Except at the two ends of the beams, where the lifting anchors were embedded, the shear reinforcement was spaced 457.2 mm (18 in) apart. Figure 31 shows a schematic drawing of a cross section of a rectangular beam. Sections A and B refer to the installation of the strands for pull-out, which is discussed further. Figure 32 shows an actual picture of the rectangular beam.

The I-shaped beams had a bottom flange width of 457 mm (18 in), a top flange width of 356 mm (14 in) a height of 1143 mm (45 in), and a web width of 150 mm (5.9 in). The reinforcement is similar as for the rectangular beams. Figure 33 shows a cross-sectional drawing of the reinforcement configuration in the I-beams.

All beams were cast from one end as the concrete truck was kept stationary at one extremity of the beam (Figure 34). The SCC was flowing through the entire formwork. The filling height at the other end of the beam varied between approximately 300 mm (1/3 of the height) to 750 mm (5/6 of the height). The truck was not moved, and once the formwork at the casting point was filled, placement was stopped for several minutes. Due to the warm weather conditions and the use of a Type III cement, thixotropy caused rapid stiffening of the concrete. A waiting time of 5 to 10 min was sufficient to allow the cast concrete to stiffen. The beam was subsequently filled with the remaining concrete, creating a casting joint or a pour line. This pour line was taken into account to drill the concrete cores and for the pull-out tests. The concrete placed on top of the pour line was necessary to allow handling of the beam, but is not used by the research team.

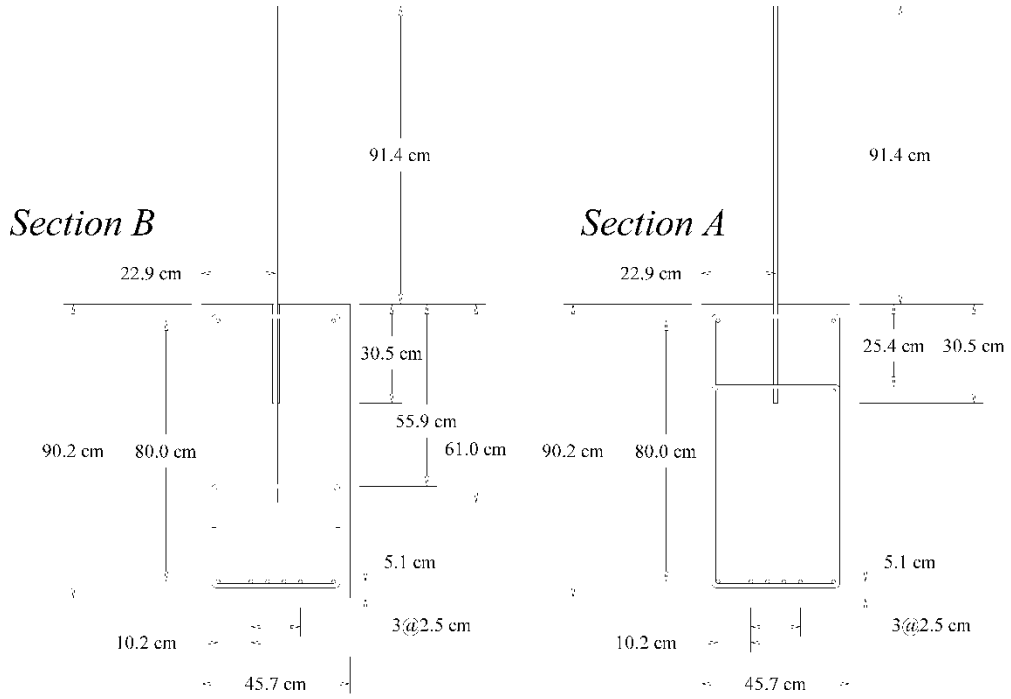

Figure 31. Reinforcement in a cross section of the rectangular beams. Sections A and B refer to the installment of the prestress strands for pull-out tests.

Figure 32. Reinforcement configuration in rectangular beams.

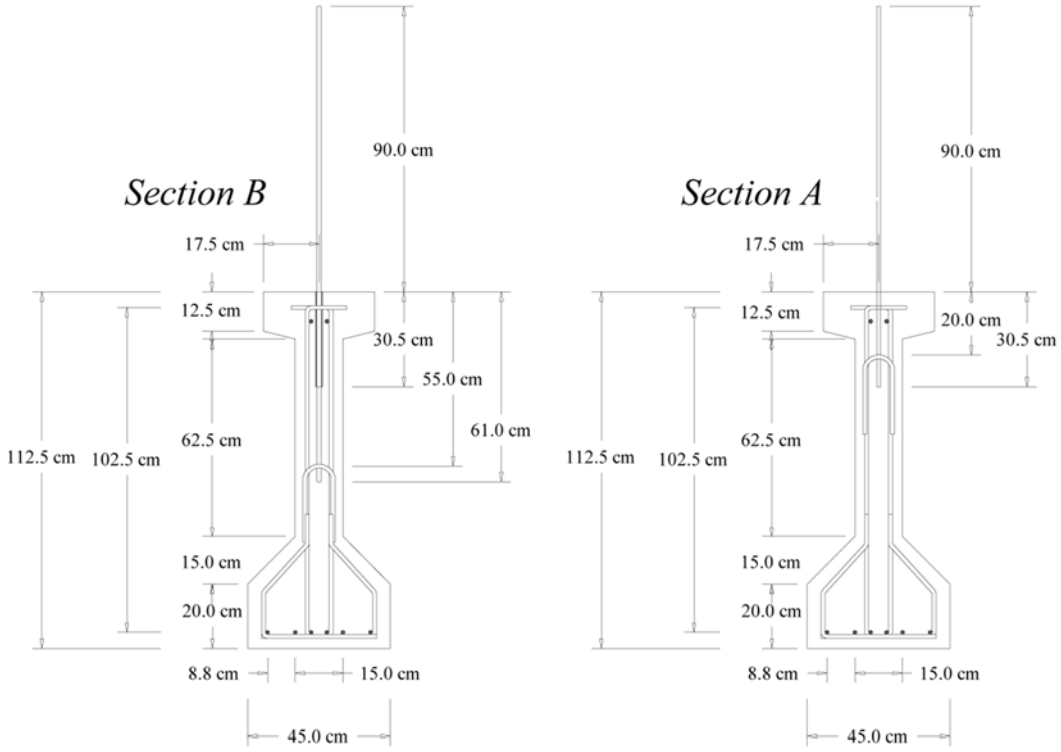

Figure 33. Cross-sectional drawing of the reinforcement of the I-beams.

Figure 34. Casting of concrete beam from one side.

4.3.2 Fresh concrete characterization

During casting of the beams, the research team received a sample from the truck to perform the following tests on fresh concrete:

- Slump flow / T50 / VSI (see section 3.3.1)
- V-Funnel flow time (see section 3.3.2)
- Density and air content (see section 3.3.3)
- Static stability by means of sieve stability (see section 3.3.4)
- Dynamic stability by means of the T-box test (see section 3.3.5). However, the number of cycles was reduced to 60, to assure the concrete did not show too much influence of the observed workability loss.
- Rheological properties by means of the ICAR Rheometer

The ICAR Rheometer is a concrete rheometer based on the principles of coaxial cylinders (similar to the ConTec 5). The inner cylinder is a 4 bladed vane, with an inner radius of 63.5 mm and a height of 127 mm. The outer cylinder is the concrete bucket and has a radius of 143 mm. The testing procedure consists of pre-shearing the sample at 0.5 rps during 20 s and applying a stepwise decrease in rotational velocity from 0.5 to 0.025 rps, in 10 steps, taking 5 s each. If torque is in equilibrium at a certain step, torque and rotational velocity are averaged during the last 4 s of each step. With the discrete data points, yield stress and plastic viscosity are calculated, employing a correction for non-zero empty measurements, and a correction for plug flow. Furthermore, after analysis of the data, the yield stress obtained by the ICAR rheometer was not fully trusted. Instead, it was calculated based on slump flow using an analytical formula [26]. The viscosity was then adjusted based on this value.

4.3.3 Ultrasonic pulse velocity (UPV) applied on the beams

Before determining the bond strength between the prestress strands and the concrete in the beams, the team of Dr. J.A. Hartell measured on-site the ultrasonic pulse velocity on beams 1, 2 and 5 (Figure 35). The test was performed using 54 kHz compressive wave sensors and the direct transmission method, according to ASTM C597. The sensors were placed perpendicular to the vertical side of the beam, directly opposite to each other. The travel time between wave emission and reception is used to calculate the wave velocity. Changes in wave velocity across the beam may indicate changes in homogeneity. The velocity measurements were performed at different heights of the beam, and at different distances from the casting point. For each point, three measurements were taken, closely to each other at the same height. An illustration of the measuring points at a certain distance from the casting points is given in Figure 36. The measurements were performed at the casting point, at 3 m (10 ft), at 6 m (20 ft) and at the end of the beam for beams 1 and 5. For beam 2, all measurements were performed at 3 m (10 ft) intervals over the entire length, except at 6 m from the casting point. The locations where the UPV measurements were performed correspond to the locations where the cores for compressive strength were drilled afterwards.

Figure 35. Dr. Hartell and her team performing the UPV measurements.

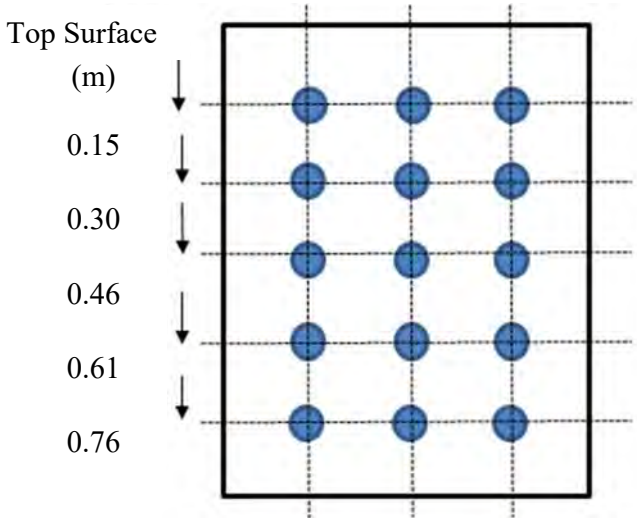

Figure 36. Spacing of measuring points at a specific distance from the casting point.

4.3.4 Bond strength between concrete and prestress strand

The bond strength between concrete and prestress strands was evaluated at three locations in the beams for 9 m (30ft) long, and in six locations for the 18 m (60ft) long beam. Strands were embedded in couples, of which one strand was attached in the top 1/3 of the height of the beam (section A in Figure 31 and Figure 33), while the other strand was embedded in the middle third of the beam height (section B in Figure 31 and Figure 33). In the latter case, the bond between the top 1/3 of the concrete height and the strand was prevented by installing plastic sleeves over the strands (Figure 32). The strands were attached to the shear reinforcement, and each pair is thus spaced 452 mm (18 in) (see Figure 32 and Figure 34 for examples).

The bond strength between the prestress strands and the cast concrete was evaluated by pulling the strand until 25 mm (1 in.) displacement was recorded. A hydraulic jack was manually operated to provide the relative displacement between the strand and the concrete, while a load cell recorded the load. The setup is shown in Figure 37.

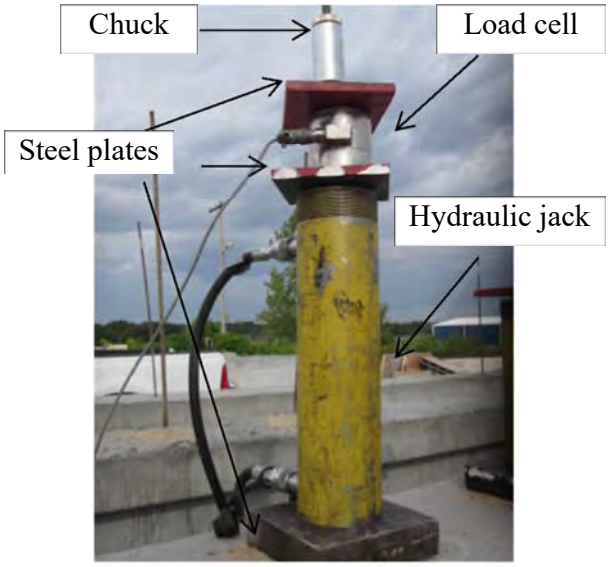

Figure 37. Setup for pull-out tests.

4.3.5 Compressive strength and ultrasonic pulse velocity on cores.

For each 9 m (30 ft) long beam, cores, 100 mm (4 in.) in diameter, were drilled from the side of the beam at 12 different locations. Over the height, the cores were taken at the bottom (just above the lower prestress strands), in the middle, and at the top. The top location was either just under the upper strand, or just below the casting line, whichever was lower. As a result, the bottom and middle cores were all taken at the same height, but the top core may have been drilled at different heights, dependent on the beam. In longitudinal direction, the cores were drilled at the casting point, at 3 m (10 ft), 6 m (20 ft) and at the end of the beam. The cores at the casting point and at the end of the beam were taken just outside the heavily reinforced lifting anchor areas. For the 18 m (60 ft) beams, the positions of the coring were similar: at the casting point, at the end, and at each 3 m (10 ft). To limit coring operations, one core was removed at each location, except at the bottom of the beam at the casting point, where three cores were drilled to assess intrinsic variations. An overview of the coring locations is shown in Figure 38.

In the laboratory, the cores were sliced into three different pieces: a 25 mm thick slice, measured from the formed surface, a 150 mm core, and another 25 mm thick slice. Both slices will be tested in the future for a visual assessment of the aggregate content and distribution, sorptivity and air-void distribution. The remaining part of the core: a 100 x 150 mm specimen (4 x 6 in.), was evaluated for ultrasonic pulse velocity and compressive strength. A correction factor was employed on the measured strength to reflect the strength on 100 x 200 mm (4 x 8 in.) cores.

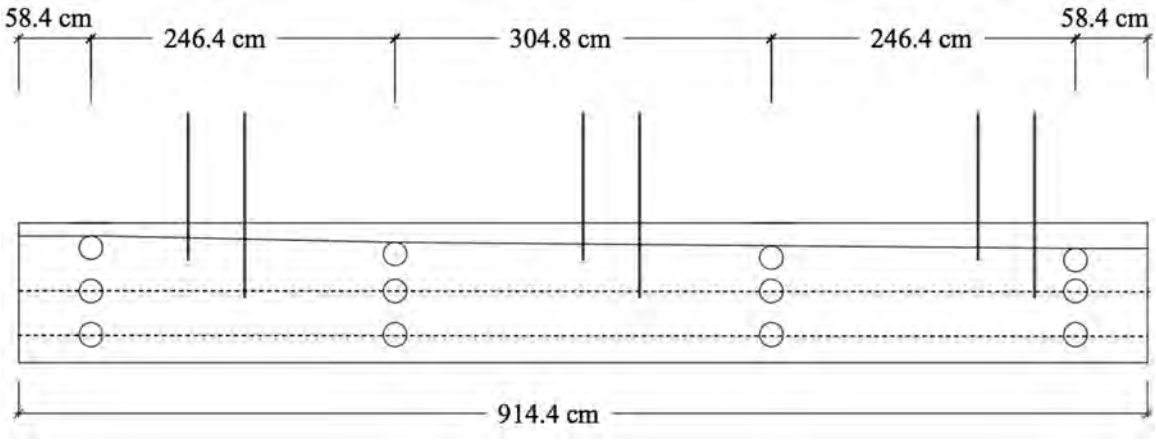

Figure 38. Example of coring locations on a 9 m (30 ft) beam. The drawing also shows the position of the strands for pullout.

4.4 Results and Discussion

4.4.1 Fresh concrete test results

Starting from the reference SCC mix design employed by Coreslab Structures, several modifications in w/cm, paste volume, admixture dosages and sand-to-total aggregate ratio were introduced to obtain different levels of workability, rheology and stability. For each 9 m (30 ft) beam, 4.6 m^3 (6 yd^3) of SCC were delivered. For beams 2 and 4, two consecutive deliveries of 4.6 m^3 (6 yd^3) and 3.8 m^3 (5 yd^3) were needed. For beam 9, all concrete was delivered in one batch. Shortly after production, the slump flow of the concrete was verified at the laboratory and the admixture dosage (HRWRA and VMA in one commercial product) was increased if necessary. After approval of the initial slump flow, the concrete was delivered to the pre-stress bed. Two wheelbarrows of SCC were sampled immediately for fresh concrete testing (see section 4.3.2) and casting was started shortly after. Table 6 summarizes the fresh properties of the concrete used in all 9 beams. All concrete mixtures were in the SCC range, as can be seen from the slump flow, T50 and V-Funnel values. By modifying the composition of the concrete, different stability levels were however achieved. The concrete mixtures delivered for beams 6 and 7 were unstable, according to the sieve stability test. These two beams also show the highest dynamic segregation indexes. From a static stability point of view, beams 1, 3, 4, 5 and 8 appear most stable. On the other hand, beams 4 and 5 have a higher dynamic segregation index. A separate discussion for each beam will not be included, but it should be noted that due to the increased w/cm in beam 4, the viscosity of the mixture is lower than all other SCC, which limited to value of the slump flow to avoid excessive segregation. Also, the mixtures for beams 5 and 9 are identical, except for the admixture content, which reduced slump flow, and the ambient temperature was also different. Beams 1-8 were produced in August, beam 9 in February. Rapid stiffening of the concrete has been noted, and with a lower temperature, the stiffening is expected to be slower for beam 9 (although no tests were performed to verify this statement). As a result, the recorded stability values may be slightly higher for beam 9, compared to its hot weather counterparts.

Table 6. Fresh properties of SCC mixtures used to cast the beams.

Beam #	Beam configuration	Mixture	**Workability**	Slump flow (mm)	Slump flow (in)	T 50 (s)	V-Funnel (s)	Air Content (%)	Sieve stability (%)	Dynamic segregation: VI in 200 mm channel	**Concrete Rheology**	Yield Stress (Pa)	Plastic Viscosity (Pa s)
1	Rect - 30ft	Ref		645	25.4	0.8	5.4	14	5.8	16.8		34.8	9.7
2	Rect - 60ft	w/cm 0.4		725	28.5	1.3	4.4	1.5	13.5	20.1		19.4	8.4
3	Rect - 30ft	Paste vol +25 l/m3		690	27.2	0.9	4.3	3	5.8	10.5		24.9	7.9
4	Rect - 60ft	w/cm 0.45		640	25.2	0.9	3.1	3.1	9.9	22.5		36.2	4.9
5	Rect - 30ft	S/A 0.56		675	26.6	0.9	2.9	10	10.3	28.1		27.7	10.2
6	I - 30 ft	Ref		630	24.8	1.3	4	13	16.6	31.3		39.2	9.1
7	I - 30 ft	Paste vol +25 l/m3		680	26.8	0.8	4.3	13	24.8	68.6		26.7	6.1
8	I - 30 ft	S/A 0.56		680	26.8	0.8	3.2	12	7.5	13		26.7	7.3
9	Rect - 60ft	S/A 0.56		660	26.0	1.6	3.6	8.5	12.9	19.7		31	15.1

4.4.2 Ultrasonic pulse velocity on the beams

One week prior to testing the bond strength of the prestress strands with the concrete, ultrasonic pulse velocity tests were performed on beams 1, 2 and 5, following the procedure described in section 4.3.3. For each distance from the casting point, and for each height, the measurement is the average of three data points, measured horizontally (as seen in Figure 36). The standard deviation of each set of three data points is very low, rendering all measured differences in pulse velocity significant. For each beam, the average of the measured pulse velocity is calculated and the percent difference from each individual point to the average is calculated. These values were then employed to create 2D color plots in Matlab, using a 3rd order polynomial fit in horizontal direction and a 2nd order polynomial in the vertical direction. These plots are displayed in Figure 39 to Figure 42. The larger the color difference in a plot, the less homogeneous the beam is. Examining the results in detail, it appears that beam 1 is the least homogeneous and beam 2 is the most uniform. The slightly less uniformity of beam 5 compared to beam 2 is expected, based on the dynamic segregation index results. However, the results on beam 1 are against the expectations and the reason for this difference still must be found.

A second conclusion which can be drawn from Figure 39 to Figure 42 is that the largest differences occur at the casting point, in vertical direction, and at the bottom of the beam in horizontal direction. This could imply that the dynamic segregation observed is more likely to be caused by the impact as the concrete has a free fall from the top of the formwork, rather than it would be fully dominated by the segregation during flow. As a result, a larger concentration of (coarse) aggregates are expected at the casting point and at the bottom of the beam, as inertia causes them to sink deeper compared to the paste.

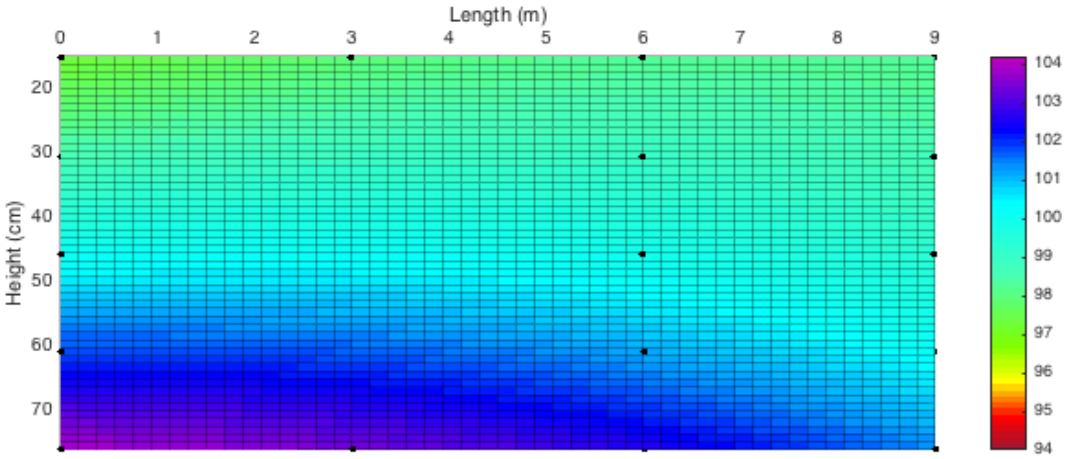

Figure 39. 2D plot of UPV results on beam 1, in percentage compared to the average value of 4130 m/s.

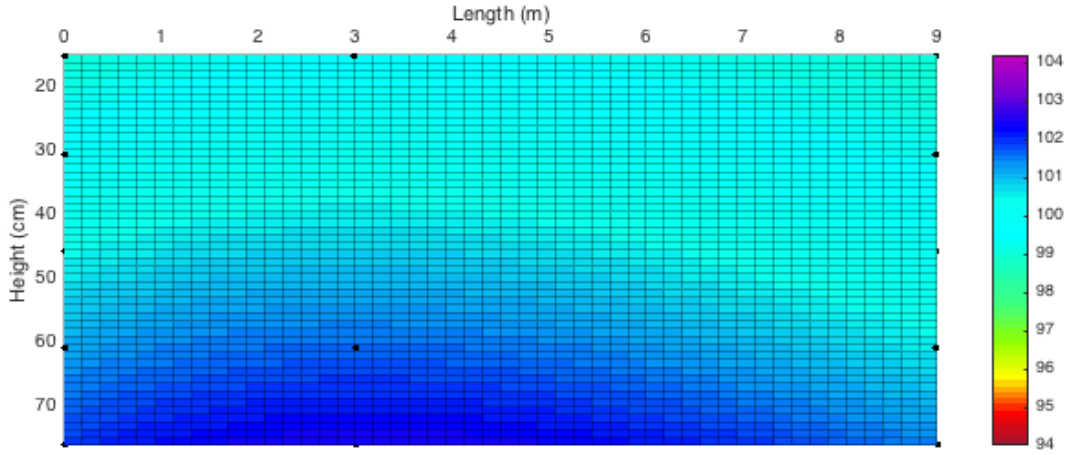

Figure 40. 2D plot of UPV results on the first 9 m (30 ft) closest to the casting point of beam 2, in percentage compared to the average value of 4602 m/s.

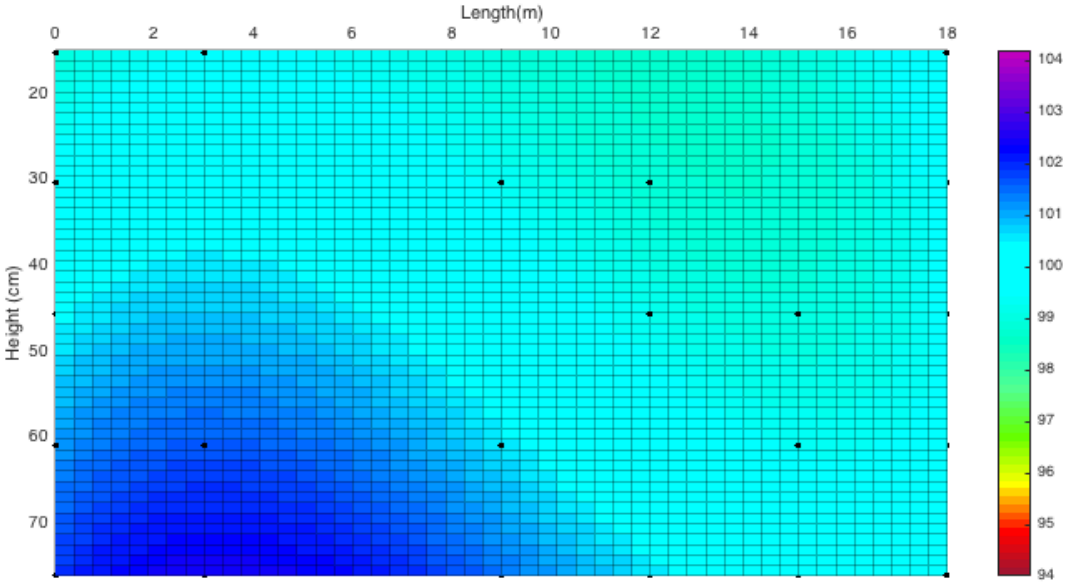

Figure 41. 2D plot of UPV results of the entire beam 2, in percentage compared to the average value of 4602 m/s.

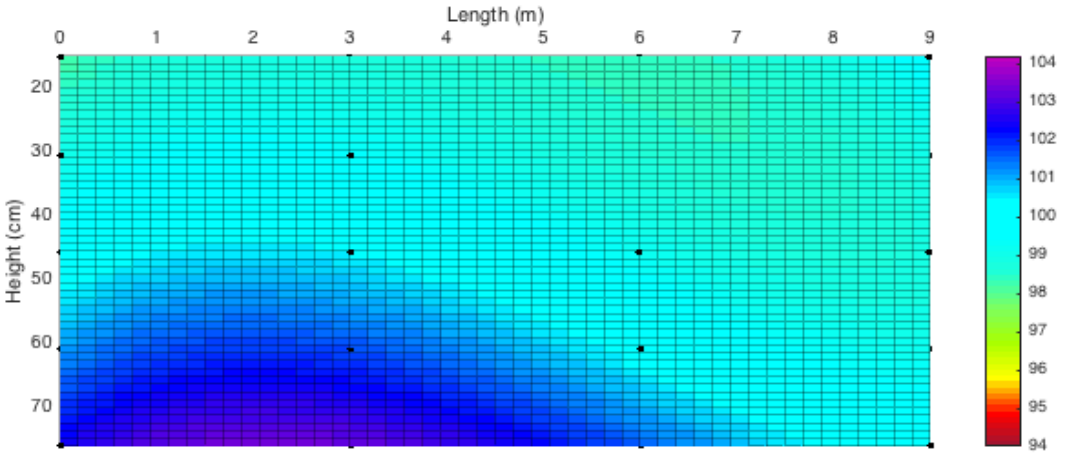

Figure 42. 2D plot of UPV results of beam 5, in percentage compared to the average value of 4311 m/s.

4.4.3 Compressive strength on cores

After extraction from the beams, the cores were transported to the laboratory for further processing. After removing the 25 mm (1 in) thick slices from the top of the core (the surface near the formwork) and the end of the core (representative for the middle of the beam), the remaining concrete specimen measured 100 x 150 mm (4 in. x 6 in.). The main purpose of this research task on the cores is to establish differences in strength within each beam, not to deliver values for acceptance or rejection of the concrete. Hence, there is no consequence of the cores being shorter than the standard L/D = 2. Furthermore, the cores were extracted more than a month after the production of the beams. The curing process of the beams, consisting of covering the beam with a plastic sheet, was stopped once the beam was removed from the formwork (at approximately 18-20 hrs after casting). Access to additional moisture during coring and cutting may lead to some additional hydration, but all cores were processed in a similar fashion, resulting in minimal differences between the cores. Furthermore, all cores of each beam were tested at the same day.

The test results are expressed in a similar fashion as the UPV results on the beams displayed in the previous section. The compressive strength values for each beam were corrected for their L/D, to reflect a L/D = 2, and to correct for any slight differences in the height of the cores. The 2D plots represent the deviation from the average core values in absolute values (in MPa, not relative). It should be noted that the results at each measuring point are based on one core. While three cores at each location would be more accurate, reliable and desired, the number of cores to be taken from the beams would have been excessive. Instead, the team has decided to remove three cores in one point of each beam (the bottom at the casting point), and take the standard deviation of these three results as a measure for significance. Typically, the standard deviations were approximately 1.5 MPa, rendering all observed results significant. Figure 43 to Figure 54 show the 2D color plots of each beam. It should be noted that a deviation of 4 MPa, represented by dark blue or bright green is equivalent to 600 psi.

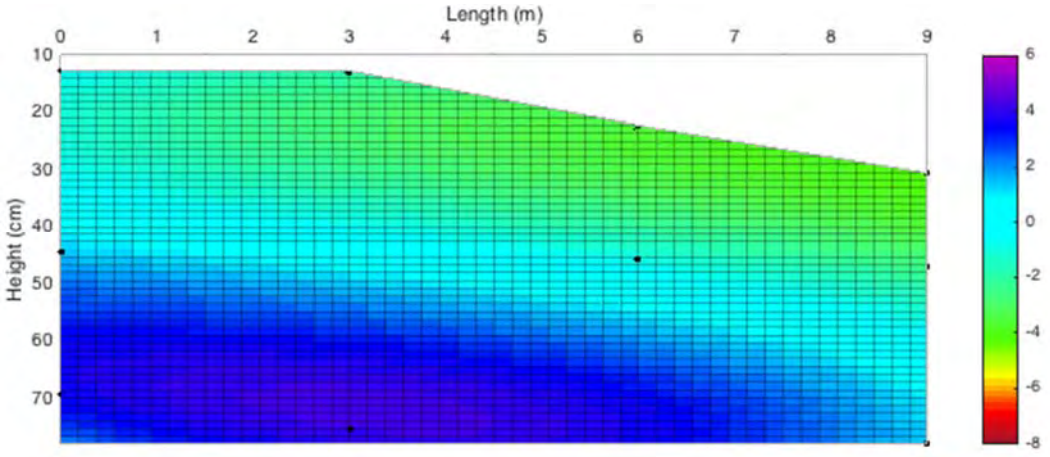

Figure 43. 2D plot of compressive strength deviation (in MPa) from the average strength (42.8 MPa, 6205 psi), for beam 1.

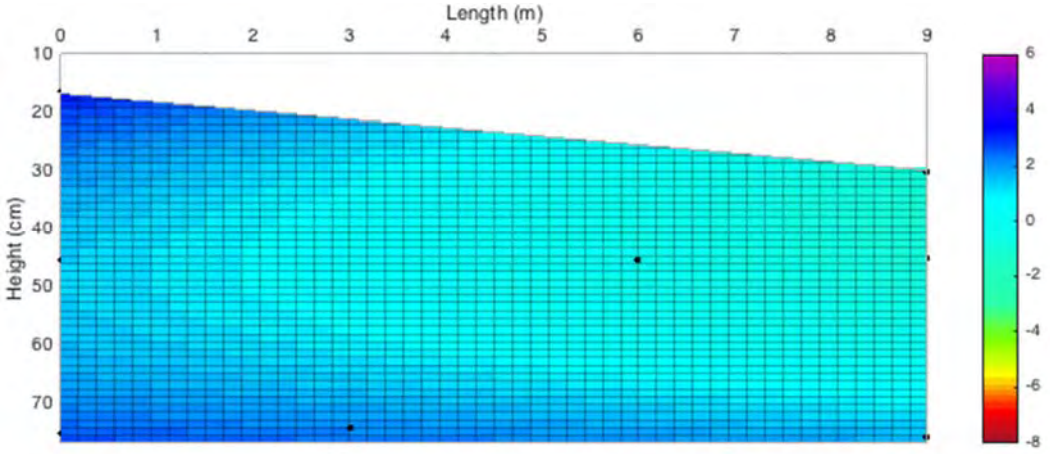

Figure 44. 2D plot of compressive strength deviation (in MPa) from the average strength (74.2 MPa, 10765 psi), in the first 9 m (30 ft) closest to the casting point for beam 2.

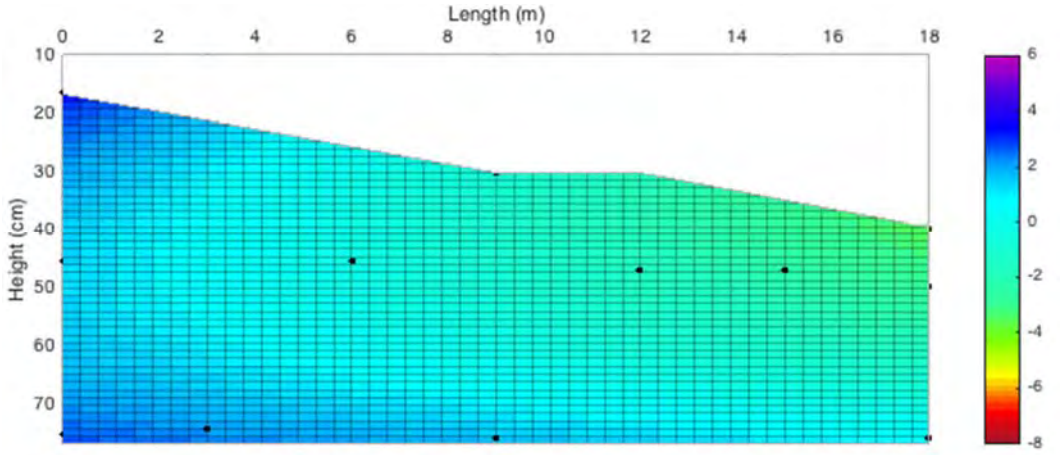

Figure 45. 2D plot of compressive strength deviation (in MPa) from the average strength (74.2 MPa, 10765 psi), for the entire beam 2.

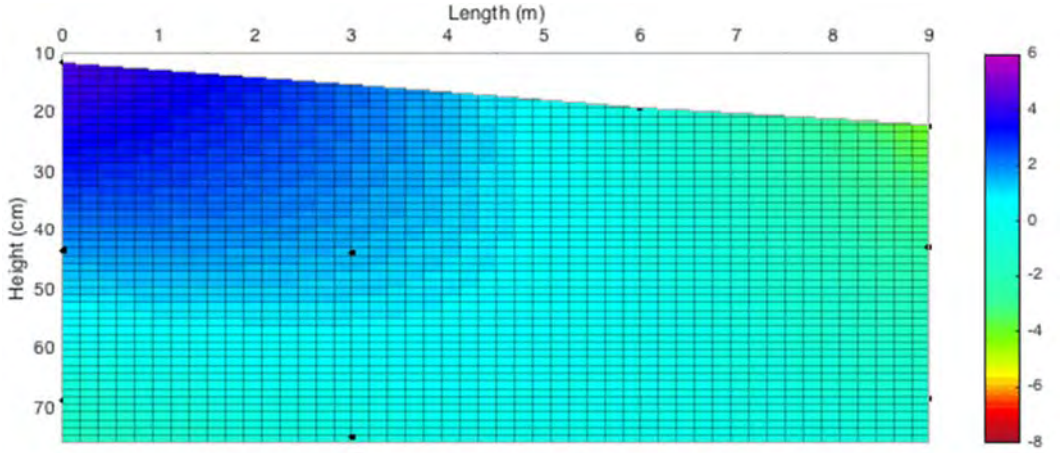

Figure 46. 2D plot of compressive strength deviation (in MPa) from the average strength (72.8 MPa, 10560 psi), for beam 3.

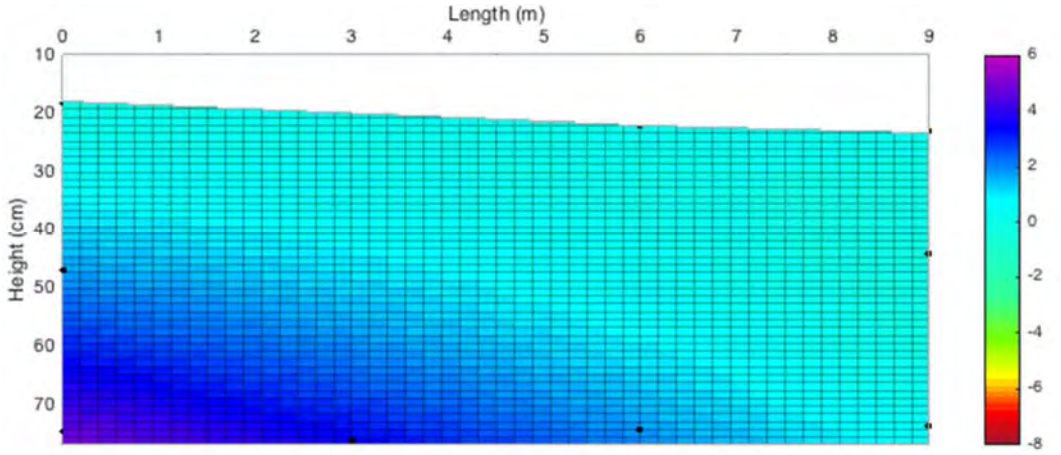

Figure 47. 2D plot of compressive strength deviation (in MPa) from the average strength (69.5 MPa, 10010 psi), in the first 9 m (30 ft) closest to the casting point for beam 4.

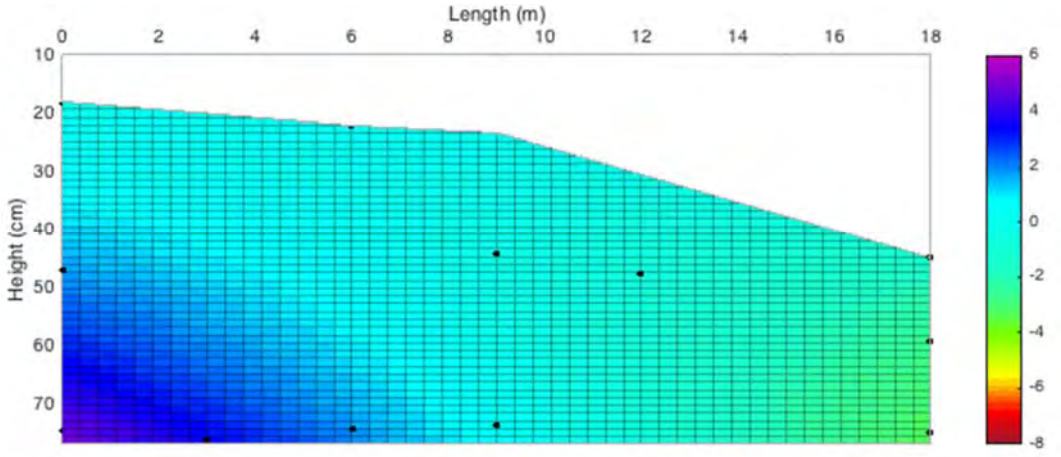

Figure 48. 2D plot of compressive strength deviation (in MPa) from the average strength (69.5MPa, 10010 psi), for the entire beam 4.

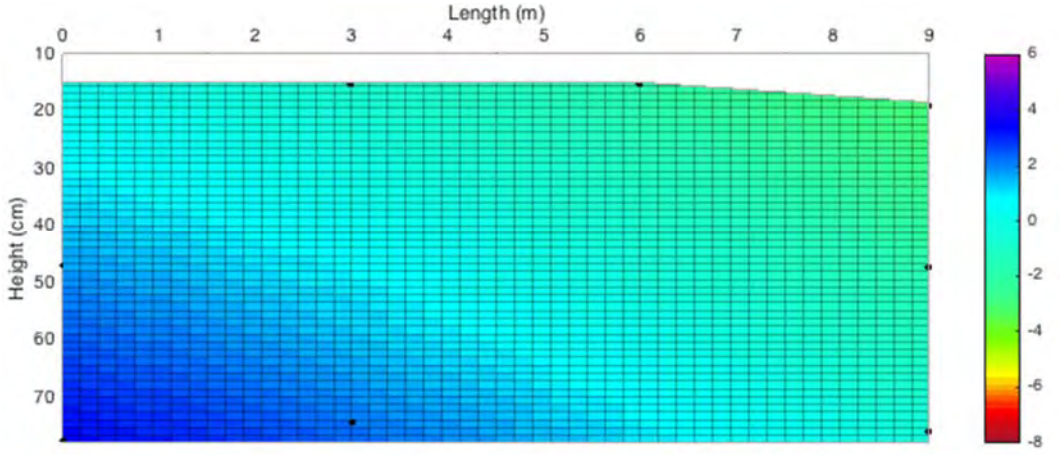

Figure 49. 2D plot of compressive strength deviation (in MPa) from the average strength (53.3 MPa, 7735 psi), for beam 5.

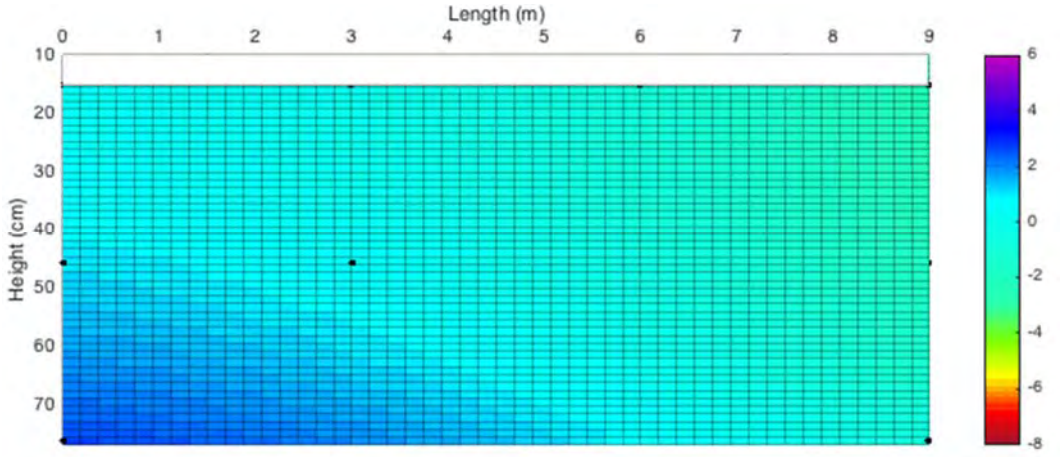

Figure 50. 2D plot of compressive strength deviation (in MPa) from the average strength (50.4 MPa, 7305 psi), for beam 6.

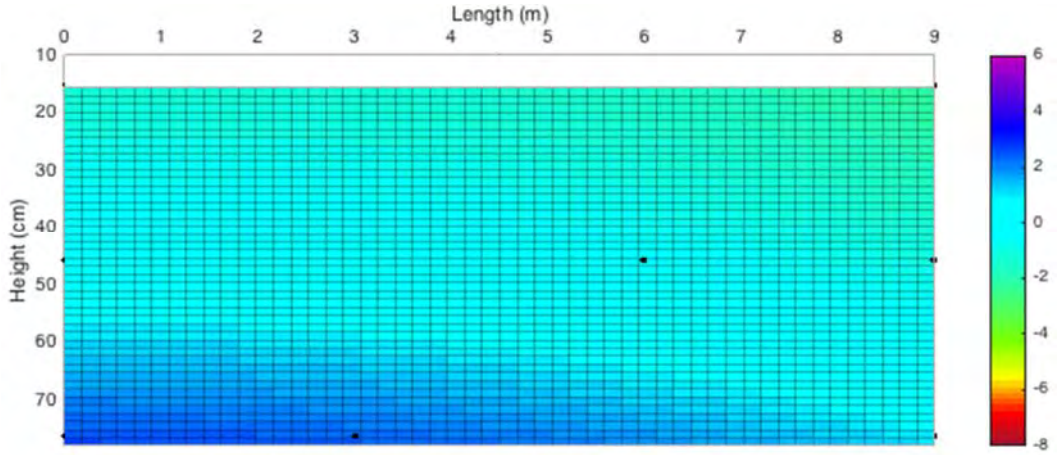

Figure 51. 2D plot of compressive strength deviation (in MPa) from the average strength (47.7 MPa, 6920 psi), for beam 7.

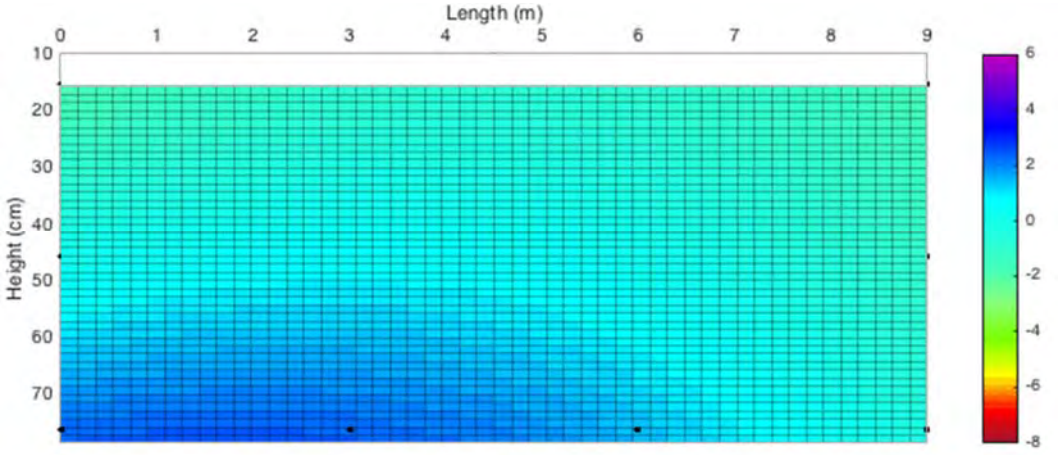

Figure 52. 2D plot of compressive strength deviation (in MPa) from the average strength (44.5 MPa, 6450 psi), for beam 8.

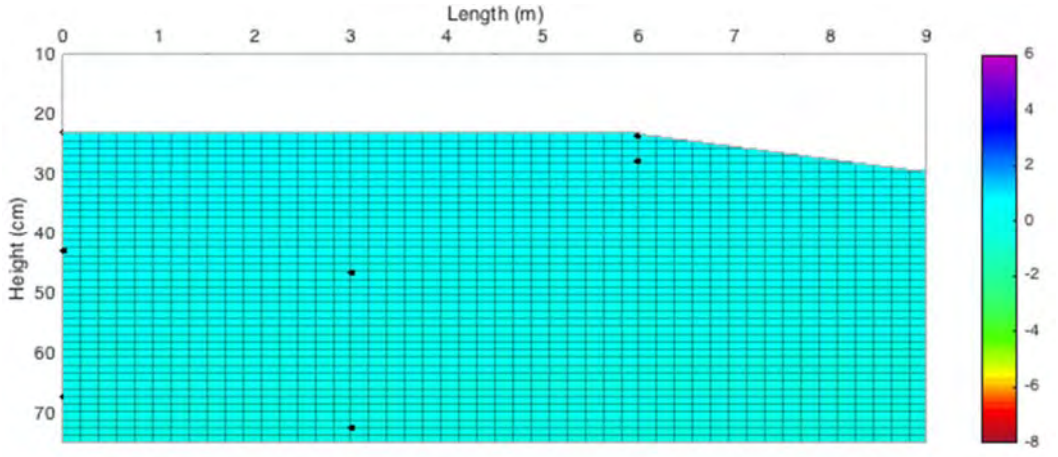

Figure 53. 2D plot of compressive strength deviation (in MPa) from the average strength (56.9 MPa, 8245 psi), in the first 9 m (30 ft) closest to the casting point for beam 9.

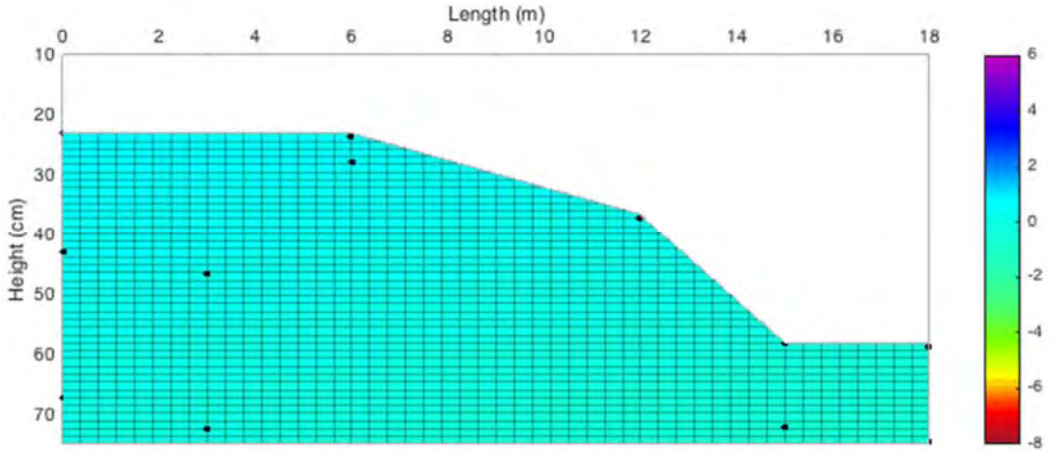

Figure 54. 2D plot of compressive strength deviation (in MPa) from the average strength (56.9MPa, 8245 psi), for the entire beam 9.

Similarly to the UPV, beam 1 shows significant non-uniformity, which is in contradiction to the expectations, based on the dynamic segregation index. Beams 2 and 3 appear quite homogeneous. Even more, the values of compressive strength on top of the beam are larger than at the bottom at the casting point. The research team is still investigating its cause. Beam 4 shows a significant increase in compressive strength at the bottom of the beam at the casting point. However, further away from that casting point, the concrete is more homogeneous, especially when comparing to beams 1, 6, 7 and 8. The SCC used for beam 4 had the highest w/cm, and thus the lowest viscosity. Low viscosity can amplify the effect of the impact during pouring of the concrete, resulting in a lower resistance by the paste or mortar to keep the coarser aggregates in suspension. Beams 6, 7 and 8 were the I-beams. As discussed in 3.4.7, a smaller width of the formwork results in less dynamic segregation. On first view, beams 6, 7 and 8 appear more stable compared to their rectangular counterparts. However, the beams are more homogeneous in horizontal direction, while in vertical direction, more non-uniformity is noted over the entire length of the beam. The SCC mixtures delivered for these beams had more static segregation issues, which is reflected in a higher compressive strength at the bottom of the beams. Beam 9 was intended for validation, minimizing the impact of dynamic segregation on the uniformity. It shows negligible segregation compared to the other beams. The detailed compressive strength results can be found in Appendix A.

To facilitate interpretation and to enable correlating uniformity of strength to any other parameter, expressing the variation in a single number is useful. For this reason, a factor $\Delta f'_c$ is developed. It expresses the difference between the compressive strength at the bottom to the compressive strength at the middle of the beam. The compressive strength is calculated as the average of all measurements at each height. The top part is not considered as the height of the specimens varied, as the SCC did not entirely fill all beams. Hence comparison between different beams is not straightforward. Figure 55 shows the relationship between $\Delta f'_c$ and the volumetric index (VI) for dynamic segregation in the 200 mm channel of the tilting box. As can be seen, a good correlation is obtained, indicating that dynamic segregation does influence the uniformity of the beam. Beam 7, which showed a VI = 68.6% was the least uniform, beam 3, with a VI of 10.5% was the most uniform, except for beam 9. However, beams 1 and 8 (hollow markers in Figure 55) showed a significantly larger $\Delta f'_c$, which cannot be correlated to the dynamic segregation index. The reason for this deviation is still under investigation. Potentially, a local change in air content may cause the different behavior.

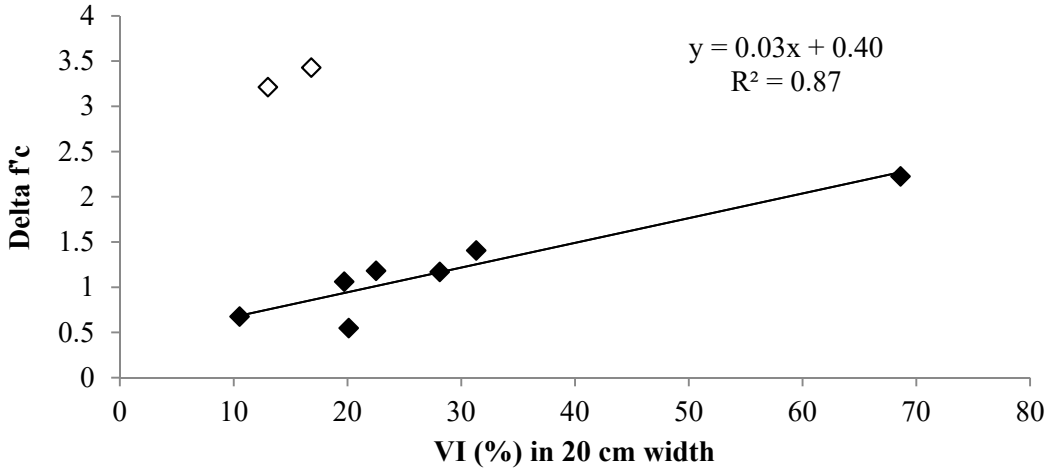

Figure 55. Relationship between uniformity of the beams and the dynamic segregation index.

4.4.4 Ultrasonic pulse velocity on the cores

Prior to crushing the core in the press, the UPV of each core was determined according to the method described in 4.3.5. The purpose of these measurements was to verify the 2D plots on compressive strength and the UPV measurements obtained on the beams. The detailed results of the UPV measurements on the cores can be found in Appendix A. On first sight, comparing the average of the UPV measured on all cores or each beam, to the average of the compressive strength of the beam, a good correlation is observed (Figure 56).

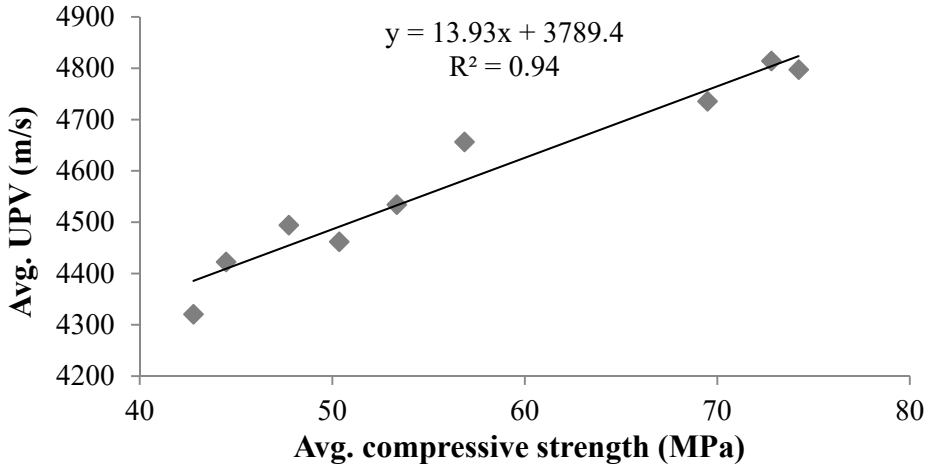

Figure 56. The average UPV on all cores correlates well with the average compressive strength of all cores for each beam.

However, considering individual results of each core, the good correlation disappears. Figure 57 shows the results from all cores. A trend is still visible between UPV and compressive strength considering all beams, but a closer look to each beam separately reveals either a weak or no correlation at all. Similarly, weak correlations between the UPV on the cores and the UPV directly measured on beams 1, 2 and 5 are observed, especially considering that the cores were extracted at the same locations as where the UPV was measured on the beams (illustrated for beam 2 in Figure 58). The reason for this discrepancy is currently unknown.

Future characterization of the remaining slices concerning aggregate content and air void distribution may clarify the cause of this behavior.

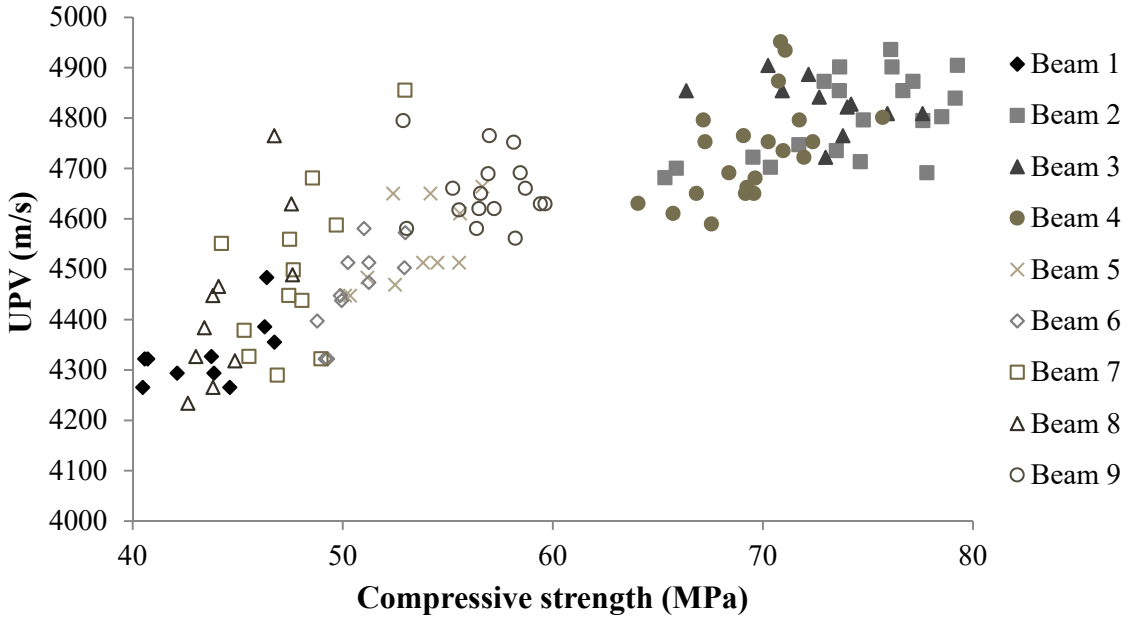

Figure 57. The individual results of UPV on each core do not correspond well to the measured compressive strength.

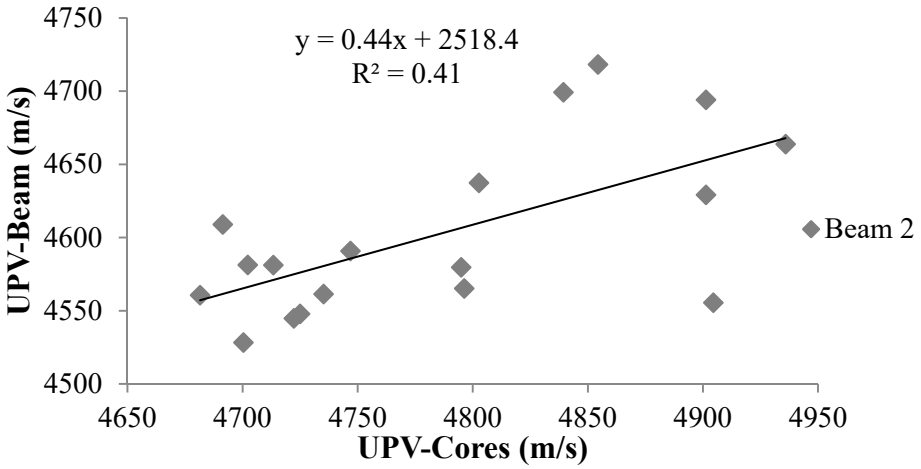

Figure 58. A weak correlation is found between the UPV on the cores and the UPV on the beams, as illustrated for beam 2.

4.4.5 Bond strength between prestress strands and concrete

The bond strength between the prestress strands and the concrete in the beams was determined according to the procedure described in section 4.3.4. For the 9 m (30 ft) beams, three pairs of strands were imbedded, for the 18 m (60 ft) beams, six pairs of strands were pulled. According to literature, bond strength measurements should be performed in horizontal direction. However, this would have resulted in drilling holes in the formworks, which was not an option. Secondly, a load-slip diagram is typically determined, and the strands are pulled until failure. Seen the manual pulling operation, pulling the strands to full loosening was too labor-

intensive. This was attempted for one strand to investigate the failure mode, and the strand slipped several times before removal. No concrete failure was recorded, neither for the one completely removed strand, neither for all other bond strength measurements.

The bond strength results are expressed as relative bond strengths, comparing the load to achieve 25 mm (1 in.) slip in the strand embedded in the top 1/3 of the beam, to the load on the strand bond to the middle 1/3 of the beam. For each beam, the average is calculated as a single number. Figure 59 shows the results for each beam. Beams 1, 3, 4 and 9 show adequate bond strength (> 80% of relative bond), while beams 5, 6, 7 and 8 showed lower than 70% bond strength in the top strand compared to its middle counterpart. Based on the comparison of the bond strength and the dynamic segregation, it is recommended to limit the dynamic segregation index to 25% to ensure adequate bond strength. Only beam 8 deviated from this recommendation. The results from beam 2 are not taken into consideration for this analysis due to illogical results.

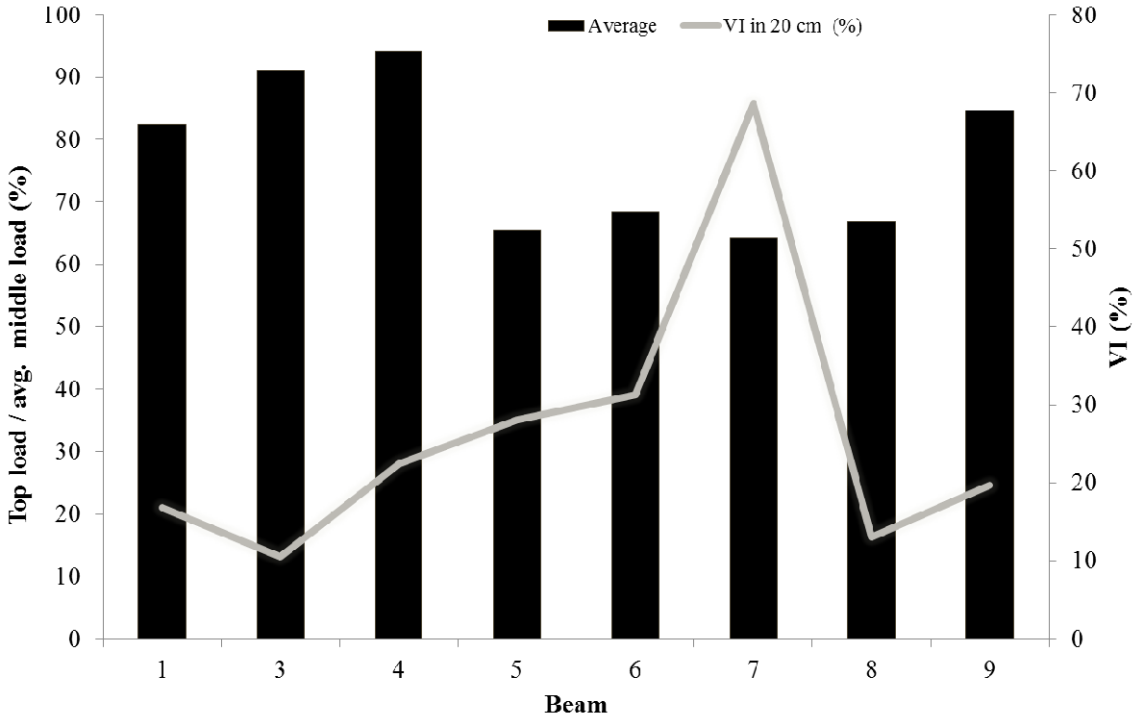

Figure 59. Relative bond strength (average of top/middle loads) for each beam, related to the dynamic segregation index.

Attempts were also made identify the change in bond strength with the distance from the casting point, but this did not deliver the expected trends. The detailed results on the loads to achieve 25 mm (1 in.) slip are included in Appendix B for the reader.

4.5 Summary and Recommendations

Based on the bond strength results, a maximum volumetric index for dynamic segregation of 25% is recommended. As a result, beams 1, 3, 4 and 9 are considered to be sufficiently dynamically stable, while the others are not. Similar conclusions can be drawn from the compressive strength results on the drilled cores, showing the largest uniformity in beams 9, 3 and 2. Furthermore, a good correlation between the dynamic segregation index and the uniformity of strength is obtained. Following the recommendation from the bond strength, the maximum difference between the compressive strength in the bottom and middle

sections of the beam should be around 1.25 MPa (180 psi), which is around the reliability of the performed measurements.

Further based on the VI ≤ 25% recommendation in the 200 mm (8 in.) channel width, the shear stress at 1 s^{-1} should be larger than 30 Pa if S/A is 0.51 or smaller, and should be larger than 40 Pa for S/A = 0.56. This means that any combination of yield stress + viscosity x 1 s^{-1}, larger than 30 Pa or 40 Pa should lead to dynamically stable SCC. However, it should be noted that these recommended values are only valid for the maximum aggregate size employed in this project (12.5 mm, 1/2 in.), as larger aggregates will result in more segregation, and that the rheological measurement on the concrete should be performed with the ConTec Viscometer 5.

It should also be noted that the criterion on dynamic segregation can be more restricted based on sorptivity and air void distribution measurements

5 Conclusions

Dynamic segregation is defined as the separation of concrete constituents (mostly coarse aggregates relative to the paste) during flow or impact. By means of the tilting box, dynamic segregation of self-consolidating concrete (SCC) can be adequately assessed. The experimental program determining the influence of different mix design factors has led to the following conclusions:

- Rheology is a major factor influencing dynamic segregation. Similarly as for static segregation, yield stress and plastic viscosity need to be balanced. High yield stress or high viscosity can prevent dynamic segregation. In this research project, the shear stress at 1 s^{-1}, which is yield stress + viscosity (x 1 s^{-1}) is found to be well related to the volumetric dynamic segregation index. The reduction in dynamic segregation caused by increasing viscosity is attributed to the increased drag force executed on the coarse aggregate. The positive influence of increasing the yield stress is assumed to be caused by an increased plugged zone, reducing the shearing effect in the concrete.
- Based on the influence of the shear stress at 1 s^{-1} on dynamic segregation, any (examined) modification in mix design which affects solely the paste composition can be explained by means of rheology. This means that increasing w/cm, increasing superplasticizer dosage, or decreasing VMA content, will increase the risk for dynamic segregation.
- Additionally to the influence of rheology, paste volume and sand-to-total aggregate ratio also affect dynamic segregation. Increasing paste volume and increasing S/A provides more space for the aggregates to move, leading to more segregation, even with constant rheological properties. Decreasing S/A also showed an increase in dynamic segregation, which is attributed to a reduction in particle lattice effect: less fine particles contribute to the stability of coarse particles. As a consequence, there is an optimum S/A for which a minimum dynamic segregation is observed. However, this optimum is expected to depend on the aggregate shape and grain size distributions.
- Smaller formwork widths, simulated by a reduction of the tilting box width from 200 mm to 100 mm reduces dynamic segregation by approximately 35%.

The second part of the project focused on evaluating the consequences of dynamic segregation on the performance of SCC. Specifically, SCC has been cast in 9 m and 18 m (30 ft and 60 ft) pre-stressed beams. The performance was evaluated by means of ultrasonic pulse velocity on beams and cores, compressive strength on cores and the bond strength of prestress strands embedded at different depths in the concrete. Other properties, such as coarse aggregate determination, sorptivity and air void distribution are still being determined on samples cored from the beams. The following conclusions can be drawn from the field tests performed at Coreslab Structures.

- From the nine beams cast, beams 1, 2, 3, 4, 8 and 9 show adequate resistance to dynamic segregation, based on the tilting box test.
- The compressive strength has been determined on cores, drilled at 3 m (10 ft) horizontal intervals and at three diffterent heights of the beam. The results show the largest variations at the casting point in the vertical direction, and at the bottom of the beam in horizontal direction. This is indicative of substantial segregation due to the impact of the SCC. In case of significant dynamic segregation, a more pronounced difference between the strength at the bottom and at the middle of the beam has been observed (see results on beams 6 and 7). However, significant variations in compressive strength in beams 1 and 8 are determined, despite the tested resistance to dynamic segregation. It is expected that variations in the air content may be the source of variation, which is undetected by the tilting box.

- UPV measurements, directly performed on beams 1, 2 and 5 confirm the conclusions deducted from the compressive strength measurements. However, the UPV measurements on the individual cores were inconclusive.
- Bond strength measurements were performed on three or six pairs of strands vertically embedded in the top 1/3 and the middle 1/3 of the height of the beams. The load necessary to obtain 25 mm (1 in.) of slip was determined. In case the dynamic segregation index was superior to 25%, the average load on the strand embedded in the top of the beam was less than 80% of the average of the strands in the middle of the beam. In case the dynamic segregation was less than 25%, this ratio was superior to 25%. Only the results of beam 8 deviate from these conclusions. Comparing the loads of individual strands as a function of the flow distance was not feasible due to the observed variation.
- Based on the observations concerning the bond strength, the acceptance value for dynamic segregation, which was suggested as 25% by Esmaeilkhanian et al., is confirmed. Therefore, it is suggested to ensure that the shear stress at 1 s^{-1} of the concrete is superior to 30 Pa in case S/A = 0.51 and 40 Pa for S/A = 0.56. However, these values may change in case larger (or smaller) aggregates or different aggregate grain size distributions are employed.
- It should also be noted that the above recommendations may be modified by the results of the sorptivity tests or the hardened air-void analyses.

Acknowledgments

The research team would like to acknowledge all parties involved in this project: Coreslab Structures in Marshall, MO by donating nine prestressed beams, including materials and personnel to execute the field work; the RE-CAST UTC for the financial support of this project; John, Jason and Brian, technical staff at the Civil, Architectural and Environmental Engineering Department and the Center for Infrastructure Engineering Studies; Sarah, Nicolas, Kristian, Saipavan, Hayder, Andrew, Shayne and Royce, all undergraduate or graduate students who have helped a hand in one or more tests; and the research team of Dr. Julie-Ann Hartell of the Oklahoma State University for the execution and interpretation of the UPV tests.

References

[1] G. De Schutter, P. Bartos, P. Domone and J. Gibbs, Self-Compacting Concrete, Caithness: Whittles Publishing, 2008.

[2] D. Panesar and B. Shindman, "The effect of segregation on transport and durability properties of self consolidating concrete," *Cement and Concrete Research,* vol. 42, pp. 252-264, 2012.

[3] H. Okamura and O. Masahiro, "Self-compacting concrete," *Journal of Advanced Concrete Technology,* vol. 1, no. 1, pp. 5-15, 2003.

[4] J. Daczko, Self-consolidating concrete: applying what we know, CRC Press, (2012).

[5] EFNARC, "The European Guidelines for Self-Compacting Concrete," 2005.

[6] S. Kosmatka and W. Panarese, "Design and control of concrete mixture.," *Portland Cement Association.,* 2004.

[7] C. Macosko, Rheology Principles, Measurements and Applications, New York: Wiley-VCH, 1994.

[8] O. Wallevik, "Rheology – A scientific tool to develop self-compacting concrete," in *Proc. of the 3rd Int. RILEM Symp. on SCC*, Reykjavik, 2003.

[9] J. Wallevik, "Rheological properties of cement paste: thixotropic behavior and structural breakdown," *Cement and Concrete Reseach,* vol. 39, pp. 14-29, 2009.

[10] J.-Y. Petit, K. Khayat and E. Wirquin, "Coupled effect of time and temperature on variations of yield value of highly flowable mortar," *Cement and Concrete Research,* vol. 36, pp. 832-841, 2006.

[11] B. Esmaeilkhanian, Dynamic stability of self-consolidating concrete: development of test methods and influencing parameters, M.Sc. thesis, Sherbrooke, QC: Universite de Sherbrooke, 2011.

[12] H. El-Chabib and M. Nehdi, "Effect of mixture design parameters on segregation of self-consolidating concrete," *ACI materials journal,* vol. 103, no. 5, pp. 374-383, 2006.

[13] A. C1610/1610M-14, "Standard Test Method for Static Segregation of Self-Consolidating Concrete Using Column Technique," 2014.

[14] A. C1611/C1611M-14, "Standard Test Method for Slump Flow of Self-Consolidating Concrete," 2014.

[15] L. Shen, L. Struble and D. Lange, "Modeling dynamic segregation of self-consolidating concrete," *ACI Materials Journal,* vol. 106, no. 4, pp. 375-380, 2009.

[16] V. K. Bui, D. Montgomery, I. Hinczak and K. Turner, "Rapid testing method for segregation resistance of self-compacting concrete," *Cement and Concrete Research,* vol. 32, no. 9, pp. 1489-1496, 2002.

[17] P. Turgut, K. Turk and H. Bakirci, "Segregation control of SCC with a modified L-box apparatus," *Magazine of Concrete Research,* vol. 64, no. 8, pp. 707-716, 2012.

[18] B. Esmaeilkhanian, D. Feys, K. Khayat and A. Yahia, "New test method to evaluate dynamic stability of-self-consolidating concrete," *ACI Materials Journal,* vol. 111, pp. 299-308, 2014.

[19] A. Ley Hernandez, Influence of mix design paranmeters on dynamic segragtion of self-consolidating concrete and consequences on performance of precast beams, M.Sc. thesis, Rolla, MO: Missouri University of Science and Technology, 2016.

[20] M. Alami, Development of a new test method to evaluate dynamic stability of self-consolidating concrete. M.Sc. Thesis, Izmir: Izmir Institute of tecnology, 2014.

[21] B. Esmaeilkhanian, K. Khayat, A. Yahia and D. Feys, "Effects of mix design parameters and rheological properties on dynamic stability of self-consolidating concrete," *Cement and Concrete Composites,* vol. 54, pp. 21-28, 2014.

[22] O. Wallevik and J. Wallevik, "Rheology as a tool in concrete science: The use of rheographs and workability boxes," *Cement and Concrete Research,* vol. 41, no. 12, pp. 1279-1288, 2011.

[23] J. Spangenberg, N. Roussel, J. Hattel, E. Sarmiento, G. Zirgulis and M. Geiker, "Patterns of gravity induced aggregate migration during casting of fluid concretes," *Cement and Concrete Research,* vol. 42, no. 12, pp. 1571-1578, 2012.

[24] J. Daczko, "Stability of self-consolidating concrete, assumed or ensured?," in *Proceedings of the First North American conference on the design and use of self-consolidating concrete*, Chicago, IL, 2002.

[25] A. C33/C33M-16, "Standard Specification for Concrete Aggregates," ASTM International, 2016.

[26] N. Roussel and P. Coussot, "“Fifty-cent rheometer” for yield stress measurements: From slump to spreading flow," *Journal of Rheology,* vol. 49, pp. 705-718, 2005.

[27] J. Daczko and M. Kurtz, "Development of High Volume Coarse Aggregate Self-Compacting Concrete," in *Proceedings of the Second International Symposium on Self-Compacting Concrete*, Tokyo, 2001.

[28] M. Geiker, M. Brandl, L. Thrane, D. Bager and O. Wallevik, "The effect of measuring procedure on the apparent rheological properties of self-compacting concrete," *Cement and Concrete Research,* vol. 32, pp. 1791-1795, 2002.

[29] J. Wallevik, Rheology of Particle Suspensions - Fresh Concrete, Mortar and Cement Paste with Various Types of Lignosulfonates. Ph-D dissertation, Trondheim: The Norwegian University of Science and Technology, 2003.

[30] O. Wallevik, D. Feys, J. Wallevik and K. Khayat, "Avoiding inaccurate interpretations of rheological measurements for cement-based materials," *Cement and Concrete Research,* vol. 78, pp. 100-109, 2015.

[31] A. C39/39M-16, "Standard Test Method for Compressive Strength of Cylindrical Concrete Specimens," ASTM International, 2016.

[32] N. Roussel, "A thixotropy model for fresh fluid concretes: theory, validation and applications," *Cement and Concrete Research,* vol. 36, no. 10, pp. 1797-1806, 2006.

Appendix A: Compressive Strength and Ultrasonic Pulse Velocity

Results on Cores

This appendix shows the results of the compressive strength and the ultrasonic pulse velocity (UPV) on the drilled cores. As the cores had an approximate length-to-diameter ratio of 1.6, a correction factor was calculated to obtain equivalent compressive strengths on cores with L/D = 2.

Table A1: UPV and compressive strength for beam 1.

Beam 1: Rectangular - 9 m / 30 ft						
Height	**Horizontal Position**		**L/D**	**UPV (m/s)**	**Corrected f'c (MPa)**	**(psi)**
Top	Casting Point		1.596	4294	42.1	6106
Middle	Casting Point		1.585	4327	43.7	6338
Bottom	Casting Point		1.599	4386	46.3	6715
Top	3 m	10 ft	1.606	4322	40.6	5889
Middle	3 m	10 ft	1.585	4266	44.6	6469
Bottom	3 m	10 ft	1.596	4355	46.7	6773
Top	6 m	20 ft	1.596	4294	39.2	5685
Middle	6 m	20 ft	1.585	4266	40.5	5874
Bottom	6 m	20 ft	1.596	4484	46.4	6730
Top	End		1.554	4241	38.7	5613
Middle	End		1.606	4322	40.7	5903
Bottom	End		1.596	4294	43.9	6367
			Average	**4321**	**42.8**	**6205**

Table A2: UPV and compressive strength for beam 2.

Beam 2: Rectangular - 18 m / 60 ft						
Height	**Horizontal Position**		**L/D**	**UPV (m/s)**	**Corrected f'c (MPa)**	**(psi)**
Top	Casting Point		1.617	4904	79.3	11502
Middle	Casting Point		1.596	4795	77.6	11255
Bottom	Casting Point		1.578	4839	79.2	11487
Top	3 m	10 ft				
Middle	3 m	10 ft	1.617	4936	76.1	11037
Bottom	3 m	10 ft	1.575	4854	73.6	10675
Top	6 m	20 ft	1.575	4854	76.7	11124
Middle	6 m	20 ft	1.606	4873	72.9	10573
Bottom	6 m	20 ft	1.606	4873	77.2	11197
Top	9 m	30 ft	1.543	4682	65.3	9471
Middle	9 m	30 ft	1.606	4796	74.8	10849
Bottom	9 m	30 ft	1.564	4901	73.7	10689
Top	12 m	40 ft	1.606	4722	69.5	10080
Middle	12 m	40 ft	1.564	4700	65.9	9558
Bottom	12 m	40 ft	1.533	4803	78.5	11385
Top	15 m	50 ft	1.596	4735	73.5	10660
Middle	15 m	50 ft	1.575	4702	70.4	10211
Bottom	15 m	50 ft	1.564	4901	76.2	11052
Top	End		1.554	4713	74.6	10820
Middle	End		1.596	4691	77.8	11284
Bottom	End		1.564	4747	71.7	10399
			Average	**4801**	**74.2**	**10765**

Table A3: UPV and compressive strength for beam 3.

Beam 3: Rectangular 9 m / 30 ft						
Height	**Horizontal Position**		**L/D**	**UPV (m/s)**	**Corrected f'c (MPa)**	**(psi)**
Top	Casting Point		1.585	4809	77.6	11255
Middle	Casting Point		1.617	4828	74.2	10762
Bottom	Casting Point		1.596	4842	71.2	10327
Top	3 m	10 ft	1.564	4822	73.8	10704
Middle	3 m	10 ft	1.575	4854	74	10733
Bottom	3 m	10 ft	1.585	4887	70.9	10283
Top	6 m	20 ft	1.585	4809	72.2	10472
Middle	6 m	20 ft	1.596	4691	75.9	11008
Bottom	6 m	20 ft				
Top	End		1.575	4854	70.2	10182
Middle	End		1.606	4722	66.3	9616
Bottom	End		1.599	4751	73	10588
			Average	**4806**	**72.7**	**10539**

Table A4: UPV and compressive strength for beam 4.

Beam 4: Rectangular 18 m / 60 ft						
Height	**Horizontal Position**		**L/D**	**UPV (m/s)**	**Corrected f'c (MPa)**	**(psi)**
Top	Casting Point		1.596	4735	71	10298
Middle	Casting Point		1.617	4753	70.3	10196
Bottom	Casting Point		1.603	4801	75.7	10979
Top	3 m	10 ft	1.606	4650	69.6	10095
Middle	3 m	10 ft	1.585	4935	71.1	10312
Bottom	3 m	10 ft	1.606	4951	70.8	10269
Top	6 m	20 ft	1.606	4796	67.2	9747
Middle	6 m	20 ft	1.617	4753	72.4	10501
Bottom	6 m	20 ft	1.617	4873	70.7	10254
Top	9 m	30 ft	1.606	4650	69.2	10037
Middle	9 m	30 ft	1.617	4753	67.2	9747
Bottom	9 m	30 ft	1.596	4691	68.4	9921
Top	12 m	40 ft	1.617	4681	69.6	10095
Middle	12 m	40 ft	1.585	4590	67.6	9805
Bottom	12 m	40 ft	1.606	4796	71.7	10399
Top	15 m	50 ft	1.606	4722	72	10443
Middle	15 m	50 ft	1.596	4663	69.2	10037
Bottom	15 m	50 ft	1.596	4765	69.1	10022
Top	End		1.606	4650	66.8	9689
Middle	End		1.617	4611	65.7	9529
Bottom	End		1.599	4630	64.1	9297
			Average	**4736**	**69.5**	**10079**

Table A5: UPV and compressive strength for beam 5.

Beam 5: Rectangular 9 m / 30 ft						
Height	**Horizontal Position**		**L/D**	**UPV (m/s)**	**Corrected f'c (MPa)**	**(psi)**
Top	Casting Point					
Middle	Casting Point		1.606	4513	55.5	8050
Bottom	Casting Point		1.603	4664	56.7	8224
Top	3 m	10 ft	1.606	4650	52.4	7600
Middle	3 m	10 ft	1.606	4513	54.5	7905
Bottom	3 m	10 ft	1.606	4650	54.2	7861
Top	6 m	20 ft	1.606	4448	50.1	7266
Middle	6 m	20 ft	1.606	4513	53.8	7803
Bottom	6 m	20 ft	1.617	4611	55.6	8064
Top	End		1.596	4484	51.2	7426
Middle	End		1.606	4448	50.3	7295
Bottom	End		1.606	4470	52.5	7614
			Average	**4542**	**53.3**	**7737**

Table A6: UPV and compressive strength for beam 6.

Beam 6: I-shape - 9 m /30 ft						
Height	**Horizontal Position**		**L/D**	**UPV (m/s)**	**Corrected f'c (MPa)**	**(psi)**
Top	Casting Point		1.606	4513	51.2	7426
Middle	Casting Point		1.606	4581	51	7397
Bottom	Casting Point		1.606	4573	53	7687
Top	3 m	10 ft	1.617	4438	49.9	7237
Middle	3 m	10 ft	1.606	4513	50.2	7281
Bottom	3 m	10 ft	1.617	4503	52.9	7673
Top	6 m	20 ft	1.606	4322	49.3	7150
Middle	6 m	20 ft	1.606	4448	49.9	7237
Bottom	6 m	20 ft	1.606	4474	51.2	7426
Top	End		1.617	4118	47.6	6904
Middle	End		1.606	4322	49.2	7136
Bottom	End		1.612	4386	48.8	7078
			Average	**4433**	**50.4**	**7303**

Table A7: UPV and compressive strength for beam 7.

Beam 7: I-shape - 9 m / 30 ft					
Height	**Horizontal Position**	**L/D**	**UPV (m/s)**	**Corrected f'c (MPa)**	**(psi)**
Top	Casting Point	1.554	4498	47.7	6918
Middle	Casting Point	1.606	4448	47.4	6875
Bottom	Casting Point	1.589	4587	49.7	7208
Top	3 m 10 ft	1.585	4327	45.5	6599
Middle	3 m 10 ft	1.627	4379	45.3	6570
Bottom	3 m 10 ft	1.585	4855	53	7687
Top	6 m 20 ft	1.617	4290	46.9	6802
Middle	6 m 20 ft	1.617	4438	48.1	6976
Bottom	6 m 20 ft	1.617	4681	48.6	7049
Top	End	1.596	4551	44.2	6411
Middle	End	1.606	4322	49	7107
Bottom	End	1.606	4681	47.5	6889
		Average	**4505**	**47.7**	**6924**

Table A8: UPV and compressive strength for beam 8.

Beam 8: I-shape - 9 m / 30 ft					
Height	**Horizontal Position**	**L/D**	**UPV (m/s)**	**Corrected f'c (MPa)**	**(psi)**
Top	Casting Point	1.585	4266	43.8	6353
Middle	Casting Point	1.585	4327	43	6237
Bottom	Casting Point	1.591	4489	47.6	6904
Top	3 m 10 ft	1.596	4234	43.3	6280
Middle	3 m 10 ft	1.606	4384	43.4	6295
Bottom	3 m 10 ft	1.575	4630	47.6	6904
Top	6 m 20 ft	1.596	4318	44.9	6512
Middle	6 m 20 ft	1.606	4448	43.8	6353
Bottom	6 m 20 ft	1.596	4765	46.7	6773
Top	End	1.596	4234	42.6	6179
Middle	End	1.585	4266	42.9	6222
Bottom	End	1.601	4466	44.1	6396
		Average	**4402**	**44.5**	**6451**

Table A9: UPV and compressive strength for beam 9.

Beam 9: Rectangular - 18 m / 60 ft						
Height	**Horizontal Position**		**L/D**	**UPV (m/s)**	**Corrected f'c (MPa)**	**(psi)**
Top	Casting Point		1.575	4630	59.4	8615
Middle	Casting Point		1.606	4650	56.6	8209
Bottom	Casting Point		1.599	4752	58.1	8427
Top	3 m	10 ft	1.596	4691	58.5	8485
Middle	3 m	10 ft	1.596	4765	57	8267
Bottom	3 m	10 ft	1.596	4795	52.9	7673
Top	6 m	20 ft	1.596	4620	57.2	8296
Middle	6 m	20 ft	1.606	4581	56.4	8180
Bottom	6 m	20 ft	1.585	4689	56.9	8253
Top	9 m	30 ft				
Middle	9 m	30 ft		No results available		
Bottom	9 m	30 ft				
Top	12 m	40 ft	1.585	4660	55.2	8006
Middle	12 m	40 ft	1.585	4660	58.7	8514
Bottom	12 m	40 ft	1.599	4561	58.2	8441
Top	15 m	50 ft				
Middle	15 m	50 ft	1.596	4620	56.5	8195
Bottom	15 m	50 ft	1.585	4618	55.5	8050
Top	End					
Middle	End		1.606	4581	53	7687
Bottom	End		1.575	4630	59.6	8644
			Average	**4656**	**56.9**	**8246**

UPV Directly on Beams

Table A10: UPV results measured directly on beam 1.

Distance from top (in)	Average Velocity (m/s)			
	Casting P	10 ft	20 ft	End
6	4000.35	4038.88	4009.38	4110.29
12	4130.12	4110.29	4067.7	4069.08
18	4116.49	4161.45	4095.56	4093.14
24	4190.65	4260.95	4146.34	4142.65
30	4267.59	3792.82	4286.26	4172.86

Table A11: UPV results measured directly on beam 2.

Distance from top (in)	Average Velocity (m/s)					
	Casting P	10 ft	30 ft	40 ft	50 ft	End
6	4555.46	4547.84	4560.63	4544.77	4561.38	4581.18
12	4579.65	4663.8	4565.16	4528.27	4581.23	4608.88
18	4629.23	4651.09	4625.22	4534.23	4553.85	4592.81
24	4655.83	4641.65	4578.92	4613.53	4528.23	4595.09
30	4699.28	4718.29	4694.09	4637.32	4629.1	4590.82

Table A12: UPV results measured directly on beam 5.

Distance from top (in)	Average Velocity (m/s)			
	Casting P	10 ft	20 ft	End
6	4228.19	4275.62	4243.93	4281.13
12	4265.12	4284.93	4263.64	4294.37
18	4317.33	4310.59	4251.78	4258.48
24	4397.66	4386.34	4307.8	4290.61
30	4397.73	4459.08	4406.07	4293

Appendix B: Bond Strength Results on Strands

Table B1: Pull-out results for beam 1.

Beam 1			
		Load for 25 mm (1 in) slip	
		kN	lbs
Casting Point	Middle	96.8	21,767
	Top	80.2	18,036
	Middle	93.3	20,967
	Top	92.5	20,795
End	Middle	100.5	22,590
	Top	66.7	14,995
Average	**Middle**	**96.9**	**21,775**
	Top	**79.8**	**17,942**

Table B2: Pull-out results for beam 3.

Beam 3			
		Load for 25 mm (1 in) slip	
		kN	lbs
Casting Point	Middle	188.1	42,284
	Top	155.5	34,953
	Middle	184.2	41,415
	Top	176.4	39,657
End	Middle	187.9	42,232
	Top	178.6	40,151
Average	**Middle**	**186.7**	**41,977**
	Top	**170.2**	**38,254**

Table B3: Pull-out results for beam 4.

Beam 4			
		Load for 25 mm (1 in) slip	
		kN	lbs
Casting Point	Middle	163.3	36,700
	Top	144.2	32,414
	Middle	193.8	43,573
	Top	181.1	40,718
	Middle	180.3	40,537
	Top	191.0	42,944
	Middle	187.3	42,117
	Top	163.9	36,844
	Middle	188.0	42,268
	Top		
End	Middle	171.9	38,650
	Top		
Average	**Middle**	**180.8**	**40,641**
	Top	**170.1**	**38,230**

Table B4: Pull-out results for beam 5.

Beam 5			
		Load for 25 mm (1 in) slip	
		kN	lbs
Casting Point	Middle	152.0	34,171
	Top	119.8	26,936
	Middle	167.6	37,678
	Top	111.7	25,113
End	Middle	155.9	35,049
	Top	79.5	17,864
Average	**Middle**	**158.5**	**35,633**
	Top	**103.7**	**23,304**

Table B5: Pull-out results for beam 6.

Beam 6			
		Load for 25 mm (1 in) slip	
		kN	lbs
Casting Point	Middle	145.3	32,661
	Top	88.0	19,782
	Middle	135.7	30,497
	Top	79.9	17,955
End	Middle	110.7	24,896
	Top	100.1	22,503
Average	**Middle**	**130.6**	**29,351**
	Top	**89.3**	**20,080**

Table B6: Pull-out results for beam 7.

Beam 7			
		Load for 25 mm (1 in) slip	
		kN	lbs
Casting Point	Middle	116.6	26,211
	Top	82.5	18,537
	Middle	133.4	29,992
	Top	71.5	16,075
End	Middle	97.1	21,828
	Top	69.2	15,556
Average	**Middle**	**115.7**	**26,010**
	Top	**74.4**	**16,723**

Table B7: Pull-out results for beam 8.

Beam 8			
		Load for 25 mm (1 in) slip	
		kN	lbs
Casting Point	Middle	Strands completely pulled out	
	Top		
	Middle	97.6	21,930
	Top	85.8	19,290
End	Middle	119.4	26,832
	Top	59.2	13,304
Average	**Middle**	**108.5**	**24,381**
	Top	**72.5**	**16,297**

Table B8: Pull-out results for beam 9.

Beam 9			
		Load for 25 mm (1 in) slip	
		kN	lbs
Casting Point	Middle	179.9	40,445
	Top	95.5	21,478
	Middle	144.4	32,454
	Top	111.2	24,998
	Middle	96.9	21,790
	Top	122.4	27,521
	Middle	106.4	23,915
	Top	134.4	30,220
	Middle	157.4	35,394
	Top		
End	Middle		
	Top		
Average	**Middle**	**137.0**	**30,800**
	Top	**115.9**	**26,055**